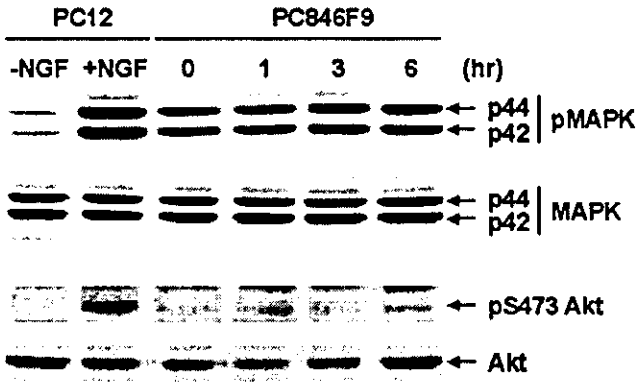

Fig. 1. Phosphorylation of MAP kinase and Akt in PC846F9 cells. Cell culture medium was changed to serum-free medium. The PC12 cells were incubated with or without NGF (25 ng/ml) for 5 min, and PC846F9 cells were collected at 0, 1, 3, and 6 hr after the medium change. Each cell lysate was subjected to SDS-PAGE (10%) and blotted onto a membrane. The membrane was incubated with anti-phospho-MAP kinase antibody, anti-MAP kinase antibody, anti-phospho-Akt antibody or anti-Akt antibody.

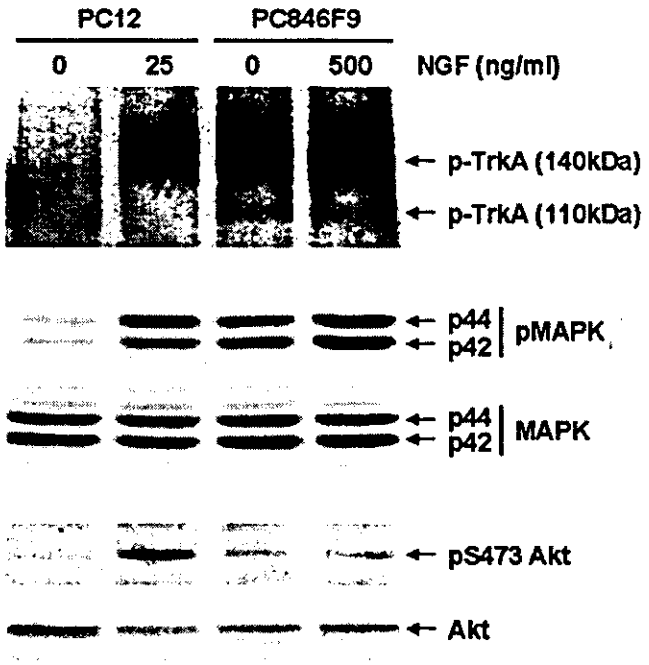

Fig. 2. Effect of high NGF concentrations on phosphorylation of TrkA, MAP kinase, and Akt in PC846F9 cells. The culture medium was changed to serum-free medium. PC12 and PC846F9 cells were incubated with or without NGF (25 and 500 ng/ml, respectively) for 5 min. Phosphorylation of TrkA was analyzed by immunoprecipitation with anti-Trk antibody and Western blotting with anti-P-Tyr antibody after electrophoresis on 7.5% acrylamide gel. Phosphorylation of MAP kinase and Akt was analyzed as described in Figure 1.

the link between p75 and the growth arrest, we examined the intracellular signaling in PC84 cells, especially the phosphorylation of MAP kinase (p44 and p42) and Akt. We focused on PC846F9 cells, one of PC84 cell subclones. The cells were incubated in serum-free medium and applied to Western blotting (Fig. 1). The MAP kinase, both p42 and p44, was phosphorylated in the PC846F9 cells, although their levels were lower than those of PC12 cells treated with NGF for 5 min. The time-dependent increase in the intensity might have been caused by the medium change at time zero. Phosphorylation of Akt was extremely low in PC846F9 cells. It remained at a low level until 6 hr after the medium change. The protein level of Akt in PC846F9 cells was comparable to that in PC12 cells (Fig. 1). These results suggest that the self-secreting NGF does not activate Akt in PC846F9 cells. When PC846F9 cells were cultured in serum containing medium, Akt was phosphorylated (data not shown). This indicates that the Akt in PC846F9 cells can be activated by another signal and PI3-kinase/Akt pathway is not damaged.

Effect of Trk Activation on Akt Activation and Growth of PC84 Cells

It is known that Akt is activated via PI3-kinase, which is activated by NGF via TrkA (Kaplan and Miller, 2000). Previously, we have shown that TrkA in PC84 cells were phosphorylated, but at a lower level than NGF-treated PC12 cells (Ito et al., 2002). This low-level activation of TrkA might have been the reason for the weak activation of Akt in PC846F9 cells. To examine this possibility, we treated PC846F9 cells with a high concentration of NGF (500 ng/ml). This treatment slightly increased the phosphorylation level of TrkA in PC846F9 cells, especially that of the 140-kDa band (Fig. 2). Under these conditions, the phosphorylation of MAP kinase was also increased, but that of Akt was not (Fig. 2). This result suggests that the contribution of TrkA to Akt activation was small in PC846F9 cells.

The morphology and growth of PC846F9 cells in the presence of the high concentration of NGF were examined. As Figure 3A shows, the cells with long processes were increased. The growth rate of PC846F9 cells was slowed down slightly by the exogenous NGF, but they continued proliferating (Fig. 3B). These results indicate that the increased activation of TrkA contributed to the morphology of the cells and the growth but it was not enough to lead to the growth arrest. The reduced activation of Akt might thus be connected to the continuous growth of PC846F9 cells.

Effect of Wortmannin on Growth Arrest of PC12 Cells

Next, we examined the possible contribution of Akt to the growth arrest in PC12 cells as in PC84 cells. To see whether the activation of PI3-kinase/Akt pathway is necessary for NGF-induced growth arrest of PC12 cells, we examined the effect of Wortmannin, an inhibitor of PI3-kinase, on the NGF-induced differentiation of PC12 cells. Pretreatment with Wortmannin reduced the phosphorylation of Akt by NGF under the serum-free condition (data not shown), and inhibited NGF-induced growth

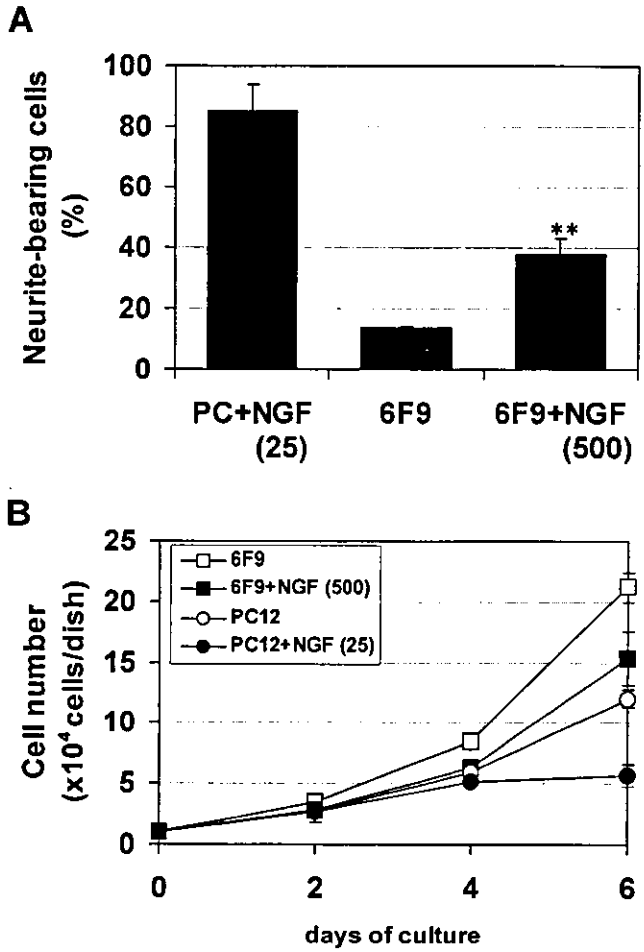

Fig. 3. Effect of high NGF concentrations on morphology and growth of PC846F9 cells. **A:** PC12 cells were treated with NGF (25 ng/ml), and PC846F9 cells were treated or not with NGF (500 ng/ml) for 6 days. Cells with processes longer than lengths equivalent to twice the size of the cell body were counted as neurite-bearing cells. The probability values were determined by Student's *t*-test: $^{**}P < 0.01$ compared with the value for PC846F9 cells. **B:** PC12 and PC846F9 cells were plated (10,000 cells per 3.5-cm dish) on Day 0. One-half of the dishes of both PC12 and PC846F9 cells were treated with NGF (25 ng/ml and 500 ng/ml, respectively) on the day. Cell numbers were counted at the indicated times.

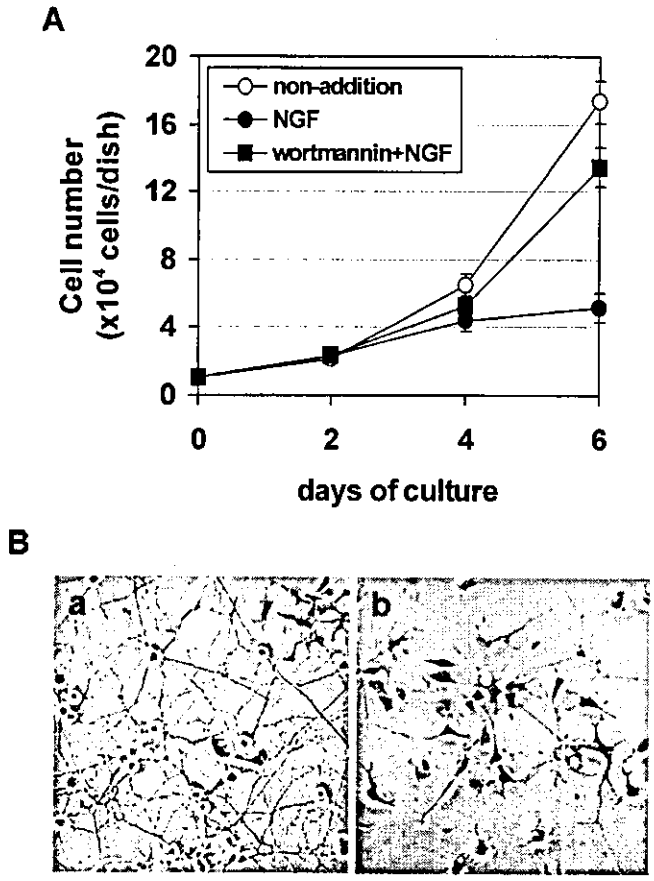

Fig. 4. Effect of Wortmannin on the differentiation of PC12 cells. **A:** PC12 cells were plated (10,000 cells per 3.5-cm dish), and pretreated the next day with Wortmannin (200 nM) for 30 min. Then NGF (25 ng/ml) was added to each dish (Day 0), and cell numbers were counted at the indicated times. **B:** morphological change of PC12 cells 6 days after the addition of NGF (25 ng/ml), with the cells preincubated with (**b**) or without (**a**) Wortmannin (200 nM).

arrest of PC12 cells in the presence of serum (Fig.4A). Moreover, the treatment with Wortmannin inhibited full extension of processes of PC12 cells (Fig. 4B). These results suggest that activation of PI3-kinase/Akt pathway was indeed essential for the NGF-induced growth arrest of PC12 cells.

Linkage Between p75 and PI3-Kinase/Akt Pathway

We have shown previously that NGF-induced growth arrest of PC12 cells was inhibited by treatment with antisense oligonucleotide of p75 or with anti-p75 neutralizing antibody (Ito et al., 2002). Next, we examined the effect of p75 repression on the phosphorylation of Akt in PC12 cells. The medium of PC12 cells was changed to serum-free medium, and the cells were incubated with anti-p75 neutralizing antibody to inhibit NGF binding to p75. This treatment significantly reduced NGF-induced phosphorylation of Akt, whereas phosphorylation of MAP kinase was not influenced (Fig. 5). Because we had observed already that this treatment made the cells unable to cease proliferation in the presence of NGF, these results suggest that the NGF activates Akt via p75 and that this activation is necessary to induce growth arrest of PC12 cells by NGF.

DISCUSSION

Previously, we showed that NGF signaling via p75 was necessary for the growth arrest of PC12 cells (Ito et al., 2002), but the downstream signaling of p75, which ultimately evoked the growth arrest, was unknown. Comparison of the intracellular signaling of PC84 and PC12 cells

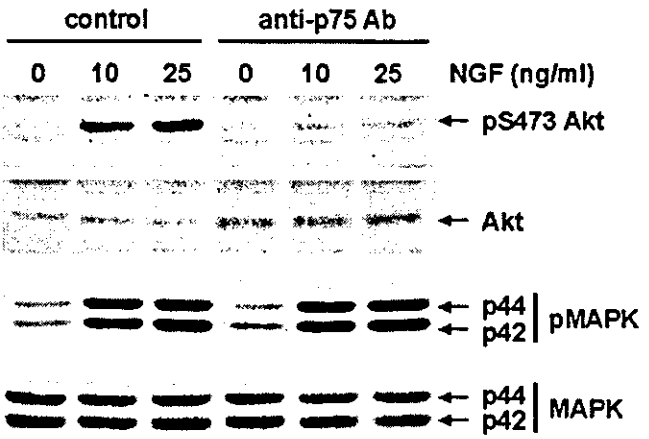

Fig. 5. Effect of repressing p75 function on phosphorylation of Akt. The medium of PC12 cells was changed to serum-free medium, and cells were pretreated with control mouse-IgG or anti-p75 neutralizing antibody for 1 hr before stimulation with NGF (0, 10, or 25 ng/ml) for 5 min. Phosphorylation of MAP kinase and Akt was analyzed as described in Figure 1.

was expected to be useful to unveil the link between p75 and the growth arrest. We found presently that MAP kinase was phosphorylated in serum-free medium but that phosphorylation of Akt was significantly low in PC846F9 cells, a subclone of PC84 cells. The phosphorylation level of TrkA and MAP kinase in PC846F9 cells was increased slightly under a high concentration of NGF, but NGF had little effect on Akt phosphorylation. Under this condition of high NGF, PC846F9 cells extended longer processes, but they did not stop proliferation. These results suggest that activation of Akt, especially via p75, was necessary for the growth arrest. The slight reduction of the growth rate when the PC846F9 cells were treated with a high NGF concentration suggests that NGF signaling via TrkA might contribute partially to the growth. The necessity of Akt activation in the growth arrest of PC12 cells was shown by the treatment with an inhibitor of PI3-kinase, Wortmannin. Further, the NGF-induced phosphorylation of Akt was repressed in PC12 cells by inhibiting NGF binding to p75 with anti-p75 antibody.

The involvement of PI3-kinase/Ak pathway in the survival of neuronal and other cell types is widely accepted (Vemuri and McMorris, 1996; Dudek et al., 1997; Crowder and Freeman, 1998), whereas its role in neuronal differentiation has not been unambiguously resolved. In this article, we suggest that activation of Akt via p75 induced the growth arrest of PC12 cells; however, Bang et al. (2001) showed that overexpression of Akt inhibited NGF-induced growth arrest and neuronal differentiation of PC12 cells (Bang et al., 2001). It was also suggested that PI3-kinase/Akt pathway might be the major mitogenic determinant in chromaffin cells (Powers et al., 1999). These reports seem contradictory to our result, but several other studies have suggested that PI3-kinase/Akt pathway had a positive role in NGF-induced neuronal differentiation of PC12 cells (Kimura et al., 1994; Jackson et al., 1996; Kobayashi et al., 1997; Kita et al., 1998). In these studies, there were differences in the degree of activation, in the duration of the activity, and in the intracellular location of Akt; in particular, some were dealing with intrinsic Akt and others with the overexpressed one. PI3-kinase was strongly activated immediately after NGF treatment and this activity declined rapidly (Kimura et al., 1994). The continuous presence of NGF, leading to the continuous activation of PI3-kinase, seemed necessary for neurite elongation. It is well known that the longevity of MAP kinase activation governs whether PC12 cells are stimulated either to proliferate or to withdraw from the cell cycle and differentiate into a neuronal phenotype (Kao et al., 2001). The differences in the activity or its duration of PI3-kinase/Akt pathway may lead to transduction of different signals, thus leading to different results. It was also reported that PI3-kinase played distinct spatial and functional roles in sympathetic neurons; activation of PI3-kinase by NGF in distal axons was more critical for survival of neurons supported by NGF than activation in cell bodies (Kuruvilla et al., 2000).

The underlying mechanism(s) for Akt-dependent control of the cell cycle is less well defined. NGF is known to induce changes in the expression level of cyclin-related proteins. It was indicated that simultaneous downregulation of cdc2 and cdk2 activity by NGF was sufficient and necessary for neuronal differentiation in PC12 cells (Dobashi et al., 1995, 2000). NGF also induced transcription of p21 and cyclin D1 in PC12 cells (Yan and Ziff, 1997), and both were reportedly activated by Akt-dependent pathway in other cells (Muise-Helmericks et al., 1998; Rössig et al., 2001). Although p21 and cyclin D1 may exert opposing effects on cell cycling, NGF can be mitogenic through cyclin D1 activity during the initial stage; and the arrest of PC12 growth coincides with the late stage, where cdk activity is inhibited by p21 (Yan and Ziff, 1997). It remains to be clarified which cyclin-related protein(s) is activated by Akt via p75 in PC12 cells and how growth arrest is introduced.

Our study has shown that p75-neutralizing antibody antagonized NGF-induced Akt phosphorylation in PC12 cells in serum-free medium, suggesting that p75 signaling induced activation of PI3-kinase/Akt pathway. It is well accepted, however, that Akt is activated by NGF via TrkA (Kaplan and Miller, 2000). Because p75 is suggested to regulate TrkA activation (Barker and Shooter, 1994), the lack of p75 function might have caused insufficient activation of Akt. Recently, however, Roux et al. (2001) indicated that low-level p75 expression facilitated cell survival more than cell death, through Akt activation via PI3-kinase-dependent pathway. It was striking that this Akt activation was independent of the ligand NGF or of TrkA. The little contribution of TrkA in Akt activation also was shown in this report, but we could not see the Akt phosphorylation without NGF in PC12 cells in serum-free medium, indicating that Akt activation was dependent on NGF. Because it has been reported that NGF promotes

activation of three isoform types of Akt in PC12 cells (Andjelkovic et al., 1998), Akt isoforms might be activated differentially by p75, by TrkA, or by both. At present, the detail with respect to isoforms is not known. It also remains to be clarified how p75 controls the PI3-kinase/Akt pathway. Roux et al. (2001) suggested a novel activation cascade of the PI3-kinase/Akt pathway by p75, including control of tyrosine phosphatase activity. They indicated that p75 expression, at least that of its cytoplasmic domain, resulted in reduced cytosolic tyrosine phosphatase activity. These points are targets of future challenging experiment.

We found that Akt in PC846F9 cells was not phosphorylated in serum-free condition but was phosphorylated in the presence of serum. There should be some difference in Akt activation between that by NGF via p75 and that by serum, where the Akt activation via p75 but not that by serum was necessary for the growth arrest. It is not clear at present the reason for the difference between the Akt activated by p75 and that activated by serum. The differential activation of Akt isoforms, as mentioned above, might explain the situation.

Finally, the study of the mutant PC84 cells has presented a new aspect in PC12 cell differentiation. NGF-dependent Akt activation via p75 may be the essential part of the mechanism responsible for the growth arrest. The details of the versatile function of Akt and its activation mechanism via p75 must be clarified in the future.

REFERENCES

Alessi DR, Andjelkovic M, Caudwell B, Cron P, Morrica N, Cohen P, Hemmings BA. 1996. Mechanism of activation of protein kinase B by insulin and IGF-1. EMBO J 15:6541–6551.

Andjelkovic M, Suidan HS, Meier R, Frech M, Allessi DR, Hemmings BA. 1998. Nerve growth factor promotes activation of the α, β and γ isoforms of protein kinase B in PC12 pheochromocytoma cells. Eur J Biochem 251:195–200.

Bang OS, Park EK, Yang SI, Lee SR, Franke TF, Kang SS. 2001. Overexpression of Akt inhibits NGF-induced growth arrest and neuronal differentiation of PC12 cells. J Cell Sci 114:81–88.

Barker PA, Shooter EM. 1994. Disruption of NGF binding to the low affinity neurotrophin receptor p75LNTR reduces NGF binding to TrkA on PC12 cells. Neuron 13:203–215.

Barrett GL, Bartlett PF. 1994. The p75 nerve growth factor mediates survival or death depending on the stage of sensory neuron development. Proc Natl Acad Sci USA 91:6501–6505.

Bellacosa A, Chan TO, Ahmed NN, Datta K, Malstrom S, Stokoe D, McCoemick F, Feng J, Tsichlis P. 1998. Akt activation by growth factors is a multiple-step process: the role of the PH domain. Oncogene 17:313–325.

Bibel M, Hoppe E, Barde YA. 1999. Biochemical and functional interactions between the neurotrophin receptors trk and p75NTR. EMBO J 18:616–622.

Carter BD, Kaltschmidt C, Kaltschmidt B, Offenhäuser N, Böhm-Matthaei R, Baeuerle PA, Barde YA. 1996. Selective activation of NF-κB by nerve growth factor through the neurotrophin receptor p75. Science 272:542–545.

Casaccia-Bonnefil P, Carter BD, Dobrowsky RT, Chao MV. 1996. Death of oligodendrocytes mediated by the interaction of nerve growth factor with its receptor p75. Nature 383:716–718.

Cross DA, Alessi DR, Cohen P, Andjelkovich M, Hemmings BA. 1995. Inhibition of glycogen synthase kinase-3 by insulin mediated by protein kinase B. Nature 378:785–789.

Crowder RJ, Freeman RS. 1998. Phosphatidylinositol 3-kinase and Akt protein kinase are necessary and sufficient for the survival of nerve growth factor-dependent sympathetic neurons. J Neurosci 18:2933–2943.

del Peso L, Gonzalez-Garcia M, Page C, Herrera R, Nunez G. 1997 Interleukin-3-induced phosphorylation of BAD through the protein kinase Akt. Science 275:687–689.

Dobashi Y, Kudoh T, Matsumine A, Toyoshima K, Akiyama T. 1995. Constitutive overexpression of CDK2 inhibits neuronal differentiation of rat pheochromocytoma PC12 cells. J Biol Chem 270:23031–23037.

Dobashi Y, Shoji M, Kitagawa M, Noguchi T, Kameya T. 2000. Simultaneous suppression of cdc2 and cdk2 activities induces neuronal differentiation of PC12 cells. J Biol Chem 275:12572–12580.

Dobrowsky RT, Werner MH, Castellino AM, Chao MV, Hannun YA. 1994. Activation of the sphingomyelin cycle through the low-affinity neurotrophin receptor. Science 265:1596–1599.

Dudek H, Datta SR, Franke TF, Birnbaum MJ, Yao R, Cooper GM, Segal RA, Kaplan DR, Greenberg ME. 1997. Regulation of neuronal survival by the serine-threonine protein kinase Akt. Science 275:661–665.

Frade JM, Barde YA. 1999. Genetic evidence for cell death mediated by nerve growth factor and the neurotrophin receptor p75 in the developing mouse retina and spinal cord. Development 126:683–690.

Franke TF, Yang SI, Chan TO, Datta K, Kazlauskas A, Morrison DK, Kaplan DR, Tsichlis PN. 1995. The protein kinase encoded by the Akt proto-oncogene is a target of the PDGF-activated phosphatidylinositol 3-kinase. Cell 81:727–736.

Furukawa S, Kamo I, Furukawa Y, Akazawa S, Satoyoshi E, Itoh K, Hayashi K. 1983. A highly sensitive enzyme immunoassay for mouse β nerve growth factor. J Neurochem 40:734–744.

Ito H, Nomoto H, Furukawa S. 2002 Role of low-affinity p75 receptor in nerve growth factor-inducible growth arrest of PC12 cells. J Neurosci Res 69:653–661.

Jackson TR, Blader IJ, Hammonds-Odie LP, Burga CR, Cooke F, Hawkins PT, Wolf AG, Heldman KA, Theibert AB. 1996. Initiation and maintenance of NGF-stimulated neurite outgrowth requires activation of a phosphoinositide 3-kinase. J Cell Sci 109:289–300.

Kao S, Jaiswal RK, Kolch W, Landreth GE. 2001. Identification of the mechanisms regulating the differential activation of the MAPK cascade by epidermal growth factor and nerve growth factor in PC12 cells. J Biol Chem 276:18169–18177.

Kaplan DR, Miller FD. 2000. Neurotrophin signal transduction in the nervous system. Curr Opin Neurobiol 10:381–391.

Kimura K, Hattori S, Kabuyama Y, Shizawa Y, Takayanagi J, Nakamura S, Toki S, Matsuda Y, Onodera K, Fukui Y. 1994. Neurite outgrowth of PC12 cells is suppressed by Wortmannin, a specific inhibitor of phosphatidylinositol 3-kinase. J Biol Chem 269:18961–18967.

Kita Y, Kimura KD, Kobayashi M, Ihara S, Kaibuchi K, Kuroda S, Ui M, Iba H, Konishi H, Kikkawa U, Nagata S, Fukkui Y. 1998. Microinjection of activated phosphatidylinositol-3 kinase induces process outgrowth in rat PC12 cells through the Rac-JNK signal transduction pathway. J Cell Sci 111:907–915.

Kobayashi M, Nagata S, Kita Y, Nakatsu N, Ihara S, Kaibuchi K, Kuroda S, Ui M, Iba H, Konishi H, Kikkawa U, Saitoh I, Fukui Y. 1997. Expression of a constitutively active phosphatidylinositol 3-kinase induces process formation in rat PC12 cells. J Biol Chem 272:16089–16092.

Kuruvilla R, Ye H, Ginty DD. 2000. Spatially and functionally distinct roles of the PI3-K effector pathway during NGF signaling in sympathetic neurons. Neuron 27:499–512.

Lewin GR, Barde YA. 1996. Physiology of neurotrophins. Annu Rev Neurosci 19:289–317.

Loeb DM, Stephens RM, Copeland T, Kaplan DR, Greene LA. 1994. A Trk nerve growth factor (NGF) receptor point mutation affecting interaction with phospholipase C-γ1 abolishes NGF-promoted peripherin induction but not neurite outgrowth. J Biol Chem 269:8901–8910.

Muise-Helmericks RC, Grimes HL, Bellacosa A, Malstrom SE, Tsichlis PN, Rosen N. 1998. Cyclin D expression is controlled post-transcriptionally via a phosphatidylinositol 3-kinase/Akt-dependent pathway. J Biol Chem 273:29864–29872.

Nomoto H, Tomotoshi K, Ito H, Furukawa S. 2000. Balance of two secretion pathways of nerve growth factor in PC12 cells changes during the progression of their differentiation, with a decrease in constitutive secretion in more differentiated cells. J Neurosci Res 59:632–642.

Obermeier A, Lammers R, Wiesmüller KH, Jung G, Schlessinger J, Ullrich A. 1993. Identification of Trk binding sites for SHC and phosphatidylinositol 3′-kinase and formation of a multimeric signaling complex. J Biol Chem 268:22963–22966.

Ohmichi M, Pang L, Decker SJ, Saltiel AR. 1992. Nerve growth factor stimulates the activities of the raf-1 and the mitogen-activated protein kinase via the trk protooncogene. J Biol Chem 267:14604–14610.

Pang L, Sawada T, Decker SJ, Saltiel AR. 1995. Inhibition of MAP kinase kinase blocks the differentiation of PC12 cells induced by nerve growth factor. J Biol Chem 270:13585–13588.

Powers JF, Shahsavari M, Tsokas P, Tischler AS. 1999. Nerve growth factor receptor signaling in proliferation of normal adult rat chromaffin cells. Cell Tissue Res 295:21–32.

Robbins DJ, Cheng M, Zhen E, Vanderbilt CA, Feig L, Cobb MH. 1992. Evidence for a Ras-dependent extracellular signal-regulated protein kinase (ERK) cascade. Proc Natl Acad Sci USA 89:6924–6928.

Rössig L, Jadidi AS, Urbich C, Badorff C, Zeiher AM, Dimmeler S. 2001. Akt-dependent phosphorylation of p21Cip1 regulates PCNA binding and proliferation of endothelial cells. Mol Cell Biol 21:5644–5657.

Roux PP, Bhakar AL, Kennedy TE, Barker PA. 2001. The p75 neurotrophin receptor activates Akt (protein kinase B) through a phosphatidylinositol 3-kinase-dependent pathway. J Biol Chem 276:23094–23104.

Rudkin BB, Lazarovici P, Levi BZ, Abe Y, Fujita K, Guroff G. 1989. Cell cycle-specific action of nerve growth factor in PC12 cells: differentiation without proliferation. EMBO J 8:3319–3325.

Rydén M, Hempstead B, Ibáñez CF. 1997. Differential modulation of neuron survival during development by nerve growth factor binding to the p75 neurotrophin receptor. J Biol Chem 272:16322–16328.

Toker A, Newton AC. 2000. Akt/protein kinase B is regulated by autophosphorylation at the hypothetical PDK-2 site. J Biol Chem 275:8271–8274.

Vemuri GS, McMorris FA. 1996. Oligodendrocytes and their precursors require phosphatidylinositol 3-kinase signaling for survival. Development 122:2529–2537.

Yan GZ, Ziff EB. 1995. NGF regulates the PC12 cell cycle machinery through specific inhibition of the Cdk kinases and induced of cyclin D1. J Neurosci 15:6200–6212.

Yan GZ, Ziff EB. 1997. Nerve growth factor induces transcription of the p21WAF1/CIP1 and cyclin D1 genes in PC12 cells by activating the Sp1 transcription factor. J Neurosci 17:6122–6132.

Available online at www.sciencedirect.com
SCIENCE DIRECT
Neuroscience Letters 364 (2004) 11–15
Neuroscience Letters
www.elsevier.com/locate/neulet

Axonal regrowth downregulates the synthesis of glial cell line-derived neurotrophic factor in the lesioned rat sciatic nerve

Yoshihisa Yamada[a,b], Katsuji Shimizu[b], Atsumi Nitta[a], Hitomi Soumiya[a], Hidefumi Fukumitsu[a], Shoei Furukawa[a,*]

[a] *Laboratory of Molecular Biology, Gifu Pharmaceutical University, Mitahora-higashi 5-6-1, Gifu 502-8585, Japan*
[b] *Department of Orthopaedic Surgery, Gifu University, Tsukasa-machi 40, Gifu 500-8705, Japan*

Received 18 December 2003; received in revised form 16 March 2004; accepted 22 March 2004

Abstract

The effect of axonal regeneration on de novo synthesis of glial cell line-derived neurotrophic factor (GDNF) in rat sciatic nerves was examined. Transection of the sciatic nerve caused a prominent increase in the GDNF content in the distal segments within 1 week. The high level was sustained until 4 weeks in the animal model in which the nerve ends were ligated with thread (non-regeneration group); however, it was reduced to the original level within 2 or 4 weeks after the transection only in the segments invaded by regenerating axons in the models in which the nerve ends were coaptated (regeneration group). Expression of both GDNF protein and mRNA was decreased with a reciprocal increase in the density of neurofilaments, used as a marker of axonal ingrowth in distal segments of the regeneration group, suggesting that axonal contact turned off the GDNF-mediated nerve regeneration activity.

Keywords: Glial cell line-derived neurotrophic factor (GDNF); Synthesis; Injury; Nerve regeneration; Sciatic nerve; Enzyme immunoassay (EIA)

Peripheral nerve regeneration comprises the formation of axonal sprouts, their outgrowth as regenerating axons, and the reinnervation of original targets; and these processes depend, predominantly on the biological actions of diffusible neurotrophic factors. Injury of peripheral nerves induces de novo synthesis of neurotrophic factors, including nerve growth factor (NGF), brain-derived neurotrophic factor (BDNF), and glial cell line-derived neurotrophic factor (GDNF), in the distal part of the injury [2,10,14,15]; and the factors thus accumulated play roles in axonal sprouting from the proximal stump, growth of these sprouts into the distal nerve segment, and their extension to the targets. A Schwann cell column is formed after removal of damaged myelin sheaths by macrophages, and it becomes an indispensable pathway for regenerating axons to grow through to the target [6]. Schwann cells and their basal lamina serve as the source of neurotrophic factors and/or the scaffold for regenerating axons through interactions with a variety of receptors and adhesion molecules [6,18]. However, the critical mechanisms by which peripheral nerve regeneration is achieved are not fully understood.

GFRα1 molecules, which are glycosyl-phosphatidylinositol-anchored receptors for GDNF, have recently pointed to additional functions of nerve regeneration. Although both GFRα1 and c-Ret, a tyrosine kinase that binds to the GFRα1–GDNF complex and transduces signals of the GDNF family, are required for responsiveness to GDNF family ligands, GFRα1 functions to capture GDNF and present it in *trans* fashion to c-Ret receptors [10]. GFRα1 elicits both long-range and localized guidance effects by creating positional information for c-Ret-expressing axons in the presence of GDNF [10]. Soluble GFRα1 can be released from cultured neurons, Schwann cells and explants of the sciatic nerve [17], and GDNF and GFRα1 mRNA expression is facilitated in the Schwann cells of the distal part of the injured sciatic nerve [5,10,15]. The coexistence of both GFRα1 and GDNF in the injured sciatic nerve strongly suggests that GFRα1–GDNF complexes predominantly facilitate nerve regeneration of c-Ret-expressing dorsal root ganglion neurons and spinal motoneurons by acting through an axonal guidance mechanism. The regulatory role of GFRα1 has been postulated from the results

* Corresponding author. Tel.: +81-58-237-3931; fax: +81-58-237-8589.
E-mail address: furukawa@gifu-pu.ac.jp (S. Furukawa).

0304-3940/$ – see front matter © 2004 Elsevier Ireland Ltd. All rights reserved.
doi:10.1016/j.neulet.2004.03.078

of detailed in vitro experiments [10], but the role of GDNF synthesis has not yet been fully evaluated.

In this study, we monitored the expression of GDNF protein and mRNA during degeneration and regeneration of the rat sciatic nerve, and found them to decrease coincidentally with the ingrowth of the regenerating axons.

All experiments with animals were carried out according to the guidelines of animal experimentation of the NIH Guide for Care and Use of Laboratory Animals. Male Wistar rats (7 weeks old, 150–180 g, Nippon SLC, Shizuoka, Japan) were divided into two groups and anesthetized with sodium pentobarbital (60 mg/kg, i.p.). In one group (non-regeneration group), the right sciatic nerve was cut distal to the obturator tendon, and both ends were ligated with 4-0 silk threads to prevent nerve regeneration. In the other group (regeneration group), the right sciatic nerve was cut at the same point, and both ends were immediately coaptated with 10-0 nylon threads under a dissecting microscope. At the appropriate time the animals were sacrificed under deep anesthesia with diethyl ether, and their sciatic nerves were dissected out and cut into six segments, each of 10-mm length. These procedures were schematically illustrated in Fig. 1.

Human recombinant GDNF was donated by Amgen (Thousand Oaks, CA, USA). GDNF (0.5 mg) dissolved in saline was emulsified with Freund's complete adjuvant and injected intradermally into rabbits four times at 2-week intervals. Blood was collected 1 week after the final injection. Specific antibodies were purified similarly as reported for anti-NGF antibodies [8], and used for coating of wells or preparation of biotinylated antibodies for enzyme immunoassay (EIA). The detection limit of our EIA system was as low as 4.0 pg/ml, dose-dependent below 1000 pg/ml, and specific for GDNF among other GDNF family proteins,

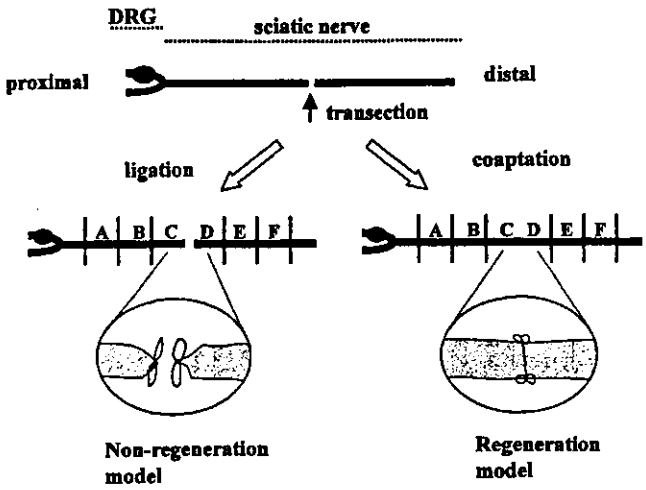

Fig. 1. A schematic representation of the location of the segments used for experiments. The sciatic nerves were dissected out and cut into six segments, each of 10-mm length. Each segment was alphabetically ordered from central to peripheral side. Transection site between segments C and D is indicated by the arrow. DRG: dorsal root ganglion.

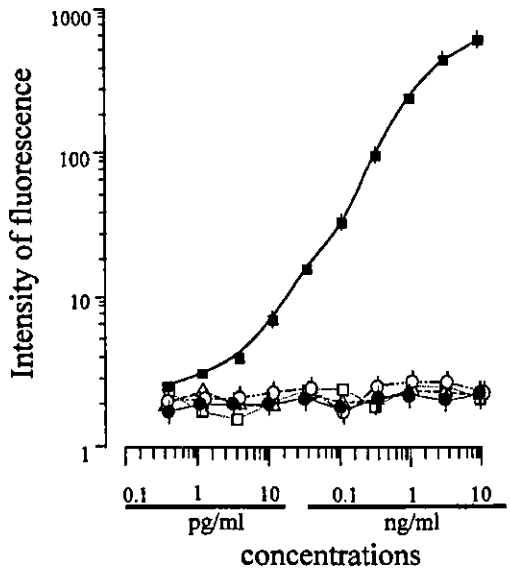

Fig. 2. Calibration curves generated for GDNF family proteins and TGF-β1 by use of the EIA system. Various concentrations of GDNF (■), neurturin (□), persephin (△), arteminm (○), and TGF-β1 (●) were applied to the EIA system for GDNF developed similarly as EIA systems for neurotrophins [16]. In short, 96-multiwell plates (Beckton Dickinson) were coated with anti-GDNF antibodies and blocked with 1% skim milk. Test samples were incubated in the antibody-coated wells. Biotinylated anti-GDNF specific antibodies were reacted with antigens bound to the wells, and these antibodies were then reacted with avidin-conjugated β-D-galactosidase (Boehringer Mannheim, Germany). Finally, the bound enzyme activity was measured by using a fluorogenic substrate, 4-methylumbelliferyl-β-D-galactoside. The standard curve of GDNF was used to determine the concentration. Each value is expressed as the mean ± S.E. of triplicate determinations. The S.E. is not shown when it is less than the width of the symbol.

including artemin, neurturin, persephin, and transforming growth factor (TGF)-β, the latter being the prototype of the super family (Fig. 2). The GDNF mRNA level was estimated by the reverse transcription-polymerase chain reaction (RT-PCR) as described earlier [7].

It was earlier shown that transection of the sciatic nerve induced a drastic increase in GDNF expression in Schwann cells located distal to the injury [5,12,15]. Neurofilaments are present in regenerating myelinated axons and larger unmyelinated axons [4], therefore, they were used as an indicator of the regenerating axons. Multiple bands of neurofilaments with about 160 kDa were found in the proximal all segments in the regeneration and non-regeneration models at all times tested. The bands appeared in the distal segments D, E, or F with the increase of the times after transection in the regeneration models, but did not in those of the non-regeneration models, demonstrating that the ingrowth of the regenerating axons occurred in the sciatic nerve of the regenerating group (Fig. 3-II). There was no difference in GDNF content between the regenerating and non-regenerating sciatic nerve up to 1 week after the surgery (Fig. 3-I). Neurofilaments were not detected in the distal stumps of either group at that time, demonstrating

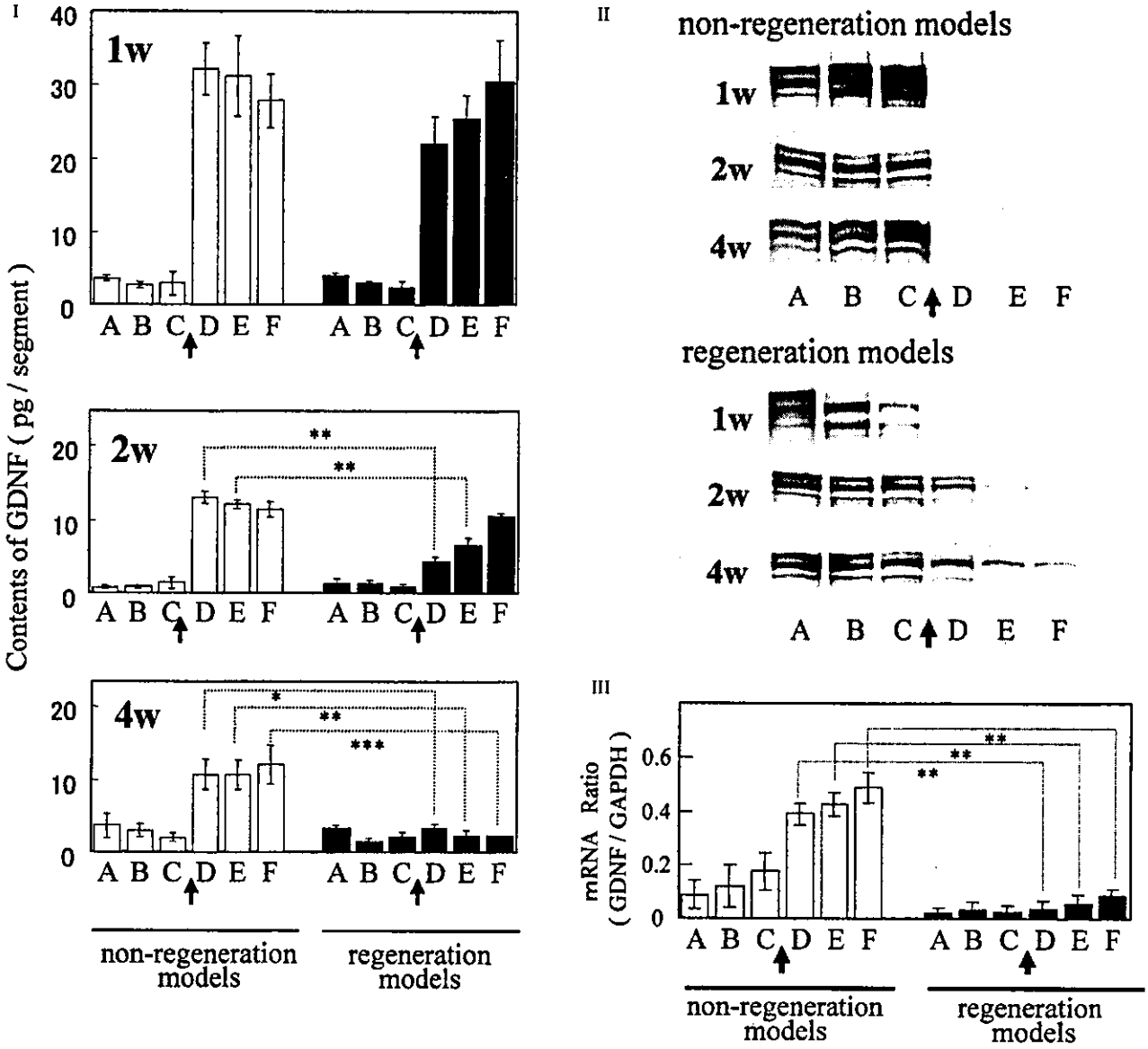

Fig. 3. Effects of nerve regeneration on the injury-induced increase in GDNF and its mRNA in the sciatic nerve segments. (I) Distribution of GDNF protein in the sciatic nerves of the regeneration (right) and non-regeneration (left) models. Each segment was pulse-sonicated in 0.1 M Tris–HCl buffer, pH 7.4, containing 1 M NaCl, 2 % bovine serum albumin, 2 mM EDTA, 80 units aprotinin/l, and 0.02% NaN_3. The supernatant fluids after centrifugation were subjected to the EIA to measure GDNF and to Western immunoblotting for neurofilaments. GDNF content is expressed as bars with the means ± S.E. of six to nine animals. Open bars indicate the values of the non-regeneration group; and closed bars, those of the regeneration group. Significance: $^{*}P < 0.05$, $^{**}P < 0.01$, $^{***}P < 0.001$ vs. the value of corresponding segment of non-regeneration group (ANOVA with Tukey post hoc). (II) Distribution of neurofilaments in the sciatic nerve segments of non-regeneration (upper) and regeneration (lower) models. The supernatant fluids of tissue homogenates were electrophoresed in an SDS polyacrylamide gel, and the proteins were then transferred to PVDF membranes (Fluorotrans™, Nihon Genetics). Neurofilaments were visualized by using anti-neurofilament 160 mouse antibody (Sigma, St. Louis, MO, USA) as described earlier [1]. The photographs shown are representatives of those of three independent experiments. (III) GDNF mRNA expression of the non-regeneration (left) and regeneration (right) models. Total RNA was transcribed into cDNAs as described previously [7]. cDNAs of GDNF and glyceraldehyde 3-phosphate dehydrogenase (GAPDH) were optimally amplified with an Advantage 2 PCR Kit (Clontech) using primers specific for GDNF [12] and GAPDH [20]. The values are the means ± S.E. of the ratio of the intensity of GDNF product to that of GAPDH product obtained from an identical RNA sample ($n = 4$). Open bars indicate the values of the non-regeneration group; and the closed bars, those of the regeneration group. Significance: $^{**}P < 0.001$ vs. the value corresponding to the segment of the non-regeneration group (ANOVA with Tukey post hoc).

no ingrowth of regenerating nerves (Fig. 3-II). The GDNF level was significantly reduced 2 weeks after the surgery in the distal segments D and E of the regeneration group, in which neurofilaments were detected. However, GDNF level was unchanged in the most distal segment, segment F, yet lacking in neurofilaments. Four weeks after the operation, the reduction in the GDNF level expanded to segment F in the regeneration group; but the GDNF level still remained high in the non-regeneration group (Fig. 3-I). The reduction in the GDNF level was limited to the distal segments

containing neurofilaments (Fig. 3-II). Furthermore, the GDNF mRNA expression was reduced in all segments D, E, and F of the regeneration group when compared with that in the same segments of the non-regeneration group (Fig. 3-III). These observations suggest that the injury-induced increase in GDNF synthesis in the distal stump is negatively regulated by interactions between regenerating axons and GDNF-producing cells, i.e., Schwann cells. A gradient of GDNF formed in the distal stump may drive more rapidly and guide more effectively the growth cones of regenerating axons to the target end tissues.

In the present study, we demonstrated that the lesion-induced enhancement of GDNF synthesis was restored to the original level coincidentally with axonal ingrowth into the distal stumps. This finding suggests that axonal contact attenuates GDNF synthesis and that the lesion-enhanced GDNF synthesis is aimed at accelerating nerve regeneration, which would explain why the GDNF synthesis is low in the proximal part of the injured nerve and in the intact peripheral nerve.

Interestingly, a recent study demonstrated that exogenous GFRα1 protein potentiated neurite outgrowth of cultured embryonic sensory or sympathetic neurons and acted as a long-range directional cue by creating positional information for c-Ret-expressing axons only in the presence of GDNF [10]. As the neurites within the sciatic nerve predominantly run from sensory neurons of the dorsal root ganglia and motoneurons of the spinal cord, most of regenerating neurites express c-Ret. Moreover, GDNF was shown to act as a peripheral signal, thereby regulating both the position of motoneurons and their muscle innervation [3]. Therefore, GDNF or GFRα1–GDNF complexes produced by Schwann cells distal to the lesion site of peripheral nerves are likely to play important roles in axonal regeneration and guidance of c-Ret-expressing neurons. Our present results, that axonal ingrowth suppressed GDNF expression, lead us to propose that the GDNF-mediated regeneration/guidance system elaborated by Schwann cells is disengaged by axonal contact with Schwann cells. This may be the first in vivo evidence that regenerating axons halt the machinery driving nerve regeneration.

The mechanisms underlying the contact behavior of Schwann cell–axon association are not yet fully understood. A recent study indicated that excitation by axons increased the number of acetylcholine receptors on Schwann cells [13]. Others showed that TGF-β, a molecule known to be released from axon terminals, upregulated expression of laminin/collagen receptor, α1β1 integrin [19], or leukemia inhibitory factor on cultured Schwann cells [11]. The involvement of TGF-β in the regulatory mechanism of GDNF gene expression may be plausible, because gene expression of α1β1 integrin or leukemia inhibitory factor is upregulated in the distal nerve stump of the injured sciatic nerves as well as GDNF expression [11,19]. Moreover, Kinameri and Matsuoka [9] reported that treatment of the Schwann cells isolated from the sciatic nerve with combination of bone morphogenetic protein-2 (BMP2) and retinoic acid (RA) dramatically induced GDNF-mRNA, while BMP2 or RA alone had no effect. They also found that in the explant culture as an in vitro lesion model, sciatic nerve segments began to express mRNA for BMP2 concomitantly with the induction of GDNF mRNA. These suggest that the Schwann cell-produced BMP2 induces GDNF after nerve injury in an autocrine fashion. Therefore, ingrowing axons may down-regulate BMP2 and/or TGF-β. However, a direct interaction between Schwann cells and ingrowth axons could not be completely excluded from a possible mechanism.

Further studies are needed to identify the molecular entities that regulate GDNF synthesis in Schwann cells in vivo; and to clarify the physiological roles of GDNF in degeneration and regeneration processes in the peripheral nervous system.

References

[1] H. Fukumitsu, Y. Furukawa, M. Tsusaka, H. Kinukawa, A. Nitta, H. Nomoto, T. Mima, S. Furukawa, Simultaneous expression of brain-derived neurotrophic factor and neurotrophin-3 in Cajal-Retzius, subplate and ventricular progenitor cells during early development stages of the rat cerebral cortex, Neuroscience 84 (1998) 115–127.

[2] H. Funakoshi, J. Frisen, G. Barbany, T. Timmusk, O. Zachrisson, V.M. Verge, H. Persson, Differential expression of mRNAs for neurotrophins and their receptors after axotomy of the sciatic nerve, J. Cell Biol. 123 (1993) 55–65.

[3] G. Haase, E. Dessaud, A. Garces, B. de Bovis, M. Birling, P. Filippi, H. Schmalbruch, S. Arber, O. deLapeyriere, GDNF acts through PEA3 to regulate cell body positioning and muscle innervation of specific motor neuron pools, Neuron 35 (2002) 893–905.

[4] S.M. Hall, A.P. Kent, R. Curtis, D. Robertson, Electron microscopic immunocytochemistry of GAP-43 within proximal and chronically denervated distal stumps of transected peripheral nerve, J. Neurocytol. 21 (1992) 820–831.

[5] A. Hoke, C. Cheng, D.W. Zochodne, Expression of glial cell line-derived neurotrophic factor family of growth factors in peripheral nerve injury in rats, Neuroreport 11 (2000) 1651–1654.

[6] C. Ide, Peripheral nerve regeneration, Neurosci. Res. 25 (1996) 101–121.

[7] H. Ito, A. Nakajima, H. Nomoto, S. Furukawa, Neurotrophins facilitate neuronal differentiation of cultured neural stem cells via induction of mRNA expression of basic helix-loop-helix transcription factors Mash1 and Math1, J. Neurosci. Res. 71 (2002) 648–658.

[8] K. Kaechi, Y. Furukawa, R. Ikegami, N. Nakamura, F. Omae, Y. Hashimoto, K. Hayashi, S. Furukawa, Pharmacological induction of physiologically active nerve growth factor in rat peripheral nervous system, J. Pharmacol. Exp. Ther. 264 (1993) 321–326.

[9] E. Kinameri, I. Matsuoka, Autocrine action of BMP2 regulates expression of GDNF-mRNA in sciatic Schwann cells, Mol. Brain Res. 117 (2003) 221–227.

[10] F. Ledda, G. Paratcha, C.F. Ibanez, Target-derived GFRalpha1 as an attractive guidance signal for developing sensory and sympathetic axons via activation of Cdk5, Neuron 36 (2002) 387–401.

[11] I. Matsuoka, A. Nakane, K. Kurihara, Induction of LIF-mRNA by TGF-beta 1 in Schwann cells, Brain Res. 776 (1997) 170–180.

[12] N. Matsushita, Y. Fujita, M. Tanaka, T. Nagatsu, K. Kiuchi, Cloning and structural organization of the gene encoding the mouse glial cell line-derived neurotrophic factor, GDNF, Gene 203 (1997) 149–157.

[13] G.V. Maximov, V.V. Revin, I.P. Grunyushkin, O.R. Kols, Role of acetylcholine in regulation of interaction between axon and

Schwann cell during rhythmic excitation of nerve fibers, Biochemistry (Moscow) 65 (2000) 431–435.
[14] M. Meyer, I. Matsuoka, C. Wetmore, L. Olson, H. Thoenen, Enhanced synthesis of brain-derived neurotrophic factor in the lesioned peripheral nerve: different mechanisms are responsible for the regulation of BDNF and NGF mRNA, J. Cell Biol. 119 (1992) 45–54.
[15] P. Naveilhan, W.M. ElShamy, P. Ernfors, Differential regulation of mRNAs for GDNF and its receptors Ret and GDNFR alpha after sciatic nerve lesion in the mouse, Eur. J. Neurosci. 9 (1997) 1450–1460.
[16] A. Nitta, M. Ohmiya, T. Jin-nouchi, A. Sometani, T. Asami, H. Kinukawa, H. Fukumitsu, H. Nomoto, S. Furukawa, Endogenous neurotrophin-3 is retrogradely transported in the rat sciatic nerve, Neuroscience 8 (1999) 679–685.
[17] G. Paratcha, F. Ledda, L. Baars, M. Coulpier, V. Besset, J. Anders, R. Scott, C.F. Ibanez, Released GFRalpha1 potentiates downstream signaling, neuronal survival, and differentiation via a novel mechanism of recruitment of c-Ret to lipid rafts, Neuron 29 (2001) 171–184.
[18] Y. Shibuya, A. Mizoguchi, M. Takeichi, K. Shimada, C. Ide, Localization of N-cadherin in the normal and regenerating nerve fibers of the chicken peripheral nervous system, Neuroscience 67 (1995) 253–261.
[19] H.J. Stewart, D. Turner, K.R. Jessen, R. Mirsky, Expression and regulation of alpha1beta1 integrin in Schwann cells, J. Neurobiol. 33 (1997) 914–928.
[20] H. Wong, W.D. Anderson, T. Cheng, K.T. Riabowol, Monitoring mRNA expression by polymerase chain reaction: the "primer-dropping" method, Anal. Biochem. 223 (1994) 251–258.

Available online at www.sciencedirect.com

SCIENCE DIRECT

Developmental Biology 275 (2004) 124–142

DEVELOPMENTAL BIOLOGY

www.elsevier.com/locate/ydbio

Retinoic-acid-concentration-dependent acquisition of neural cell identity during in vitro differentiation of mouse embryonic stem cells

Yohei Okada[a,b,c], Takuya Shimazaki[a,c], Gen Sobue[b], Hideyuki Okano[a,c,*]

[a]*Department of Physiology, Keio University School of Medicine, Shinjuku-ku, Tokyo 160-8582, Japan*
[b]*Department of Neurology, Nagoya University Graduate School of Medicine, Showa-ku, Nagoya 466-8550, Japan*
[c]*Core Research for Evolutional Science and Technology (CREST), Japan Science and Technology Agency, Kawaguchi, Saitama 332-0012, Japan*

Received for publication 11 February 2004, revised 19 July 2004, accepted 21 July 2004
Available online 8 September 2004

Abstract

Retinoic acid (RA) is one of the most important morphogens, and its embryonic distribution correlates with neural differentiation and positional specification in the developing central nervous system. To investigate the concentration-dependent effects of RA on neural differentiation of mouse embryonic stem cells (ES cells), we investigated the precise expression profiles of neural and regional specific genes by ES cells aggregated into embryoid bodies (EBs) exposed to various concentrations of RA or the BMP antagonist Noggin. RA promoted both neural differentiation and caudalization in a concentration-dependent manner, and the concentration of RA was found to regulate dorso-ventral identity, i.e., higher concentrations of RA induced a dorsal phenotype, and lower concentrations of RA induced a more ventral phenotype. The induction of the more ventral phenotype was due to the higher expression level of the N-terminus of sonic hedgehog protein (Shh-N) when treated with low concentration RA, as it was abrogated by an inhibitor of Shh signaling, cyclopamine. These findings suggest that the concentration of RA strictly and simultaneously regulates the neuralization and positional specification during differentiation of mouse ES cells and that it may be possible to use it to establish a strategy for controlling the identity of ES-cell-derived neural cells.

Keywords: Embryonic stem cells; Neural differentiation; Retinoic acid; Sonic hedgehog; N-terminus of Sonic hedgehog; Positional identity; Motor neuron; Morphogen

Introduction

Embryonic stem cells (ES cells) are clonal cell lines derived from the inner cell mass (ICM) of developing blastocysts and under appropriate conditions are capable of proliferating extensively and generating various cell types derived from the three primary germ layers of the embryo in vitro. This pluripotency of ES cells provides a powerful in vitro model for investigating the mechanisms that control differentiation in early embryonic development. The basic strategy for in vitro differentiation usually adopted is to induce cell aggregation into so-called embryoid bodies (EBs) through suspension culture in nonadhesive dishes or hanging drops. Different inducing conditions during EB formation can drastically affect the proportions of the various cell types that differentiate in EBs. For example, exposure to high-concentration RA strongly drives neural induction, whereas low-concentration RA induces cardiomyocyte differentiation (Rohwedel et al., 1999). Because neural cells represent only a small percentage of cells in EBs cultured in the presence of fetal bovine serum (FBS) and the absence of an exogenous inducer, efficient generation of neural cells requires an additional inductive stimulus or other differentiation method.

There are two major strategies for generating neural cells from mouse ES cells: EB formation and serum-free direct induction. The former includes treatment with high-concentration RA (Bain et al., 1995; Fraichard et al., 1995; Strubing et al., 1995), which has been shown to promote

* Corresponding author. Department of Physiology, Keio University, School of Medicine, 35 Shinanomachi, Shinjuku-ku, Tokyo 160-8582, Japan. Fax: +81 3 3357 5445.
E-mail address: hidokano@sc.itc.keio.ac.jp (H. Okano).

0012-1606/$ - see front matter © 2004 Elsevier Inc. All rights reserved.
doi:10.1016/j.ydbio.2004.07.038

neural gene expression and repress mesodermal gene expression (Bain et al., 1996), and serum-free culture after EB formation, which enables selection of neural cells (Okabe et al., 1996). Direct induction methods consist of a co-culture system with stromal cell line PA6 as a neural inducer that has been found to have stromal-cell-derived inducing activity (SDIA) (Kawasaki et al., 2000), a low-cell-density neural stem cell (NSC) culture (neurosphere culture) with growth factors (Tropepe et al., 2001), and an adherent monolayer culture method (Ying et al., 2003).

Sequences of events leading to lineage commitment similar to those in vivo are often observed with all of these culture strategies, and, for example, exposure to Noggin or other manipulations that inhibit bone morphogenetic protein (BMPs) signaling, which blocks neural differentiation in the early development, facilitates neural differentiation of ES cells also in vitro (Finley et al., 1999; Gratsch and O'Shea, 2002; Kawasaki et al., 2000; Tropepe et al., 2001).

During the development of the mammalian central nervous system (CNS), the differentiation properties of neural stem cells (NSCs) vary depending on the stage at which they are generated (temporal identity) and their location (positional identity). These properties define the induction and sequential rounds of neurogenesis and gliogenesis, which seem to be regulated by both intrinsic and extrinsic factors, and limit their plasticity (Temple, 2001). Depending on their location, their differentiation is usually regulated by secreting signals that modulate the rostrocaudal or dorso-ventral axis of the body and by regional cues that define the borders of each CNS segment (Hitoshi et al., 2002; Temple, 2001). In view of these characteristics of NSCs, the temporal and positional identity of NSCs derived from ES cells may be controlled in vitro by the conditions under which they differentiate, the same as specification in vivo. Indeed, much interest has been focused on the generation of specific types of neurons or neural progenitors from ES cells by producing these identities with inductive signals, such as fibroblast growth factor (FGF) 8 and Shh, or with SDIA for dopaminergic neurons (Kawasaki et al., 2000, 2002; Kim et al., 2002; Lee et al., 2000; Ying et al., 2003), RA and Shh for motor neurons (Renoncourt et al., 1998; Wichterle et al., 2002), and a combination of SDIA and BMPs for dorsal and neural-crest-derived cells (Mizuseki et al., 2003).

RA is well known as the biologically active form of vitamin A and has been shown to play an important role during embryogenesis (Ross et al., 2000). RA influences neural development in the early stage of CNS development and is required to establish patterned territories of cell groups, which, for example, has been observed in rostrocaudal axis formation, according to the distribution of RA in experiments on *Xenopus* (Blumberg et al., 1997; Sive et al., 1990) and mice (Kessel, 1992; Kessel and Gruss, 1991; Marshall et al., 1992). For these reasons, RA has been thought to be one of the most important extrinsic inductive signals that can be used for neural differentiation of mouse ES cells in vitro. However, its overall effects have yet to be clearly identified, and precise analysis of alterations of gene expression caused by RA treatment should be useful for establishing proper culture protocols for the differentiation of ES cells. In the present study, we demonstrated that RA promotes neural differentiation and caudalization in a concentration-dependent manner, and that the concentration of RA affects dorso-ventral positional identity, by determining the precise gene expression profiles during differentiation of ES cells.

Materials and methods

ES cell culture

Mouse ES cells (EB3) were maintained and used for induction. ES cells were grown on gelatin-coated (0.1%) tissue culture dishes in standard ES-cell culture medium containing GMEM (Sigma G6148) supplemented with 10% FBS, glutamine (2 mM), nonessential amino acids (0.1 mM), sodium pyruvate (1 mM), 2-mercaptoethanol (2-ME) (0.1 mM), sodium bicarbonate (3 mM), HEPES (5 mM), and mLIF. EB3 is a subline derived from E14tg2a ES cells (Hooper et al., 1987) that was generated by targeted integration of Oct3/4-IRES-BSD-pA vector (Niwa et al., 2000) into the *Oct3/4* allele, and it was maintained in the medium containing 10 μg/ml blasticidin S to eliminate differentiated ES cells.

Differentiation of ES cells

For embryoid body (EB) formation, ES cells were detached and dissociated into single cells with 0.25% trypsin–EDTA and then plated onto a bacteriological dish (Kord-Valmark™) in 10 ml of αMEM (Gibco 11900-024) supplemented with 10% FBS, sodium bicarbonate (3 mM), and 0.1 mM 2-ME (EB medium) at a density of 5×10^4 cells/ml. On day 2, various concentrations of all-*trans*-retinoic acid (RA: Sigma R 2625) were added to the culture medium (2−/4+ protocol). RA was reconstituted with 100% ethanol to prepare a stock solution. It should be noted that the effective RA concentrations at which ES cells grow into EBs may be considerably higher than those indicated in the text, because FBS contains significant levels of RA. Furthermore, cells within EBs may produce endogenous RA, possibly as a secondary effect of the initially added RA. However, we used conditions in which FBS did not contain exogenous RA as a negative control (stated control in the figures), and evaluated the results in terms of relative concentrations of RA. Recombinant mouse Sonic Hedgehog (Shh) protein (amino-teminal peptide) (Shh-N; R&D Systems Inc., 461-SH) and cyclopamine (0.1 μM, 1 μM, Toronto Research Chemicals Inc., C988400) were also added on day 2 of the experiment. For Noggin treatment, 10% (v/v) culture supernatant of Cos7

cells transfected with *Xenopus* Noggin/MC BOS (a gift of Y. Takahashi) (Kohyama et al., 2001; Tonegawa and Takahashi, 1998) (xNoggin conditioned medium) was added.

EBs were collected at day 6 of culture and allowed to settle to the bottom of the tube for a few minutes. The cells were then washed once with PBS and incubated with 0.25% trypsin–EDTA for 5 min at 37°C. The enzymatic reaction was quenched by addition of an equal volume of EB medium, and the cells were dissociated with a transfer pipette by triturating 30 times. The cells were then washed twice with serum-free αMEM and resuspended in Media hormone mix (MHM) medium, which contains DMEM/F-12 (1:1) (Gibco 12100-046, 21700-075), glucose (0.6%), glutamine (2 mM), sodium bicarbonate (3 mM), HEPES (5 mM), insulin (25 μg/ml), transferrin (100 μg/ml), progesterone (20 nM), sodium selenate (30 ng), and putrescine (60 nM) (all from Sigma except for DMEM/F-12) as described previously (Shimazaki et al., 2001). The dissociated EBs were plated on poly-L-ornithine/fibronectin-coated 10-mm cover glasses (Matsunami) at a cell density of 1.6×10^5 cells/0.75 cm^2 on a 48-well culture plate (Coaster) and allowed to differentiate for 24 h.

To clarify the effects of RA added at different points in time or of exposure for different periods of culture, ES cells were differentiated into EBs based on 2−/2+/2−, 2−/2+/2+ and 4−/4+ protocols (Suppl. Fig. 1). In the 2−/2+/2− and 2−/2+/2+ protocol, various concentrations of RA were added on day 2, and on day 4 the culture medium was replaced with freshly prepared medium containing the same concentrations of RA (2−/2+/2+ protocol) or no RA (2−/2+/2− protocol). In the 4−/4+ protocol, various concentrations of RA were added to the culture medium on day 4. Total RNA was isolated at day 0, 2, 4, 6, and 8 and processed for RT-PCR analysis.

Immunocytochemistry

Dissociated EBs were cultured for 24 h and fixed with 4% paraformaldehyde for 20 min at room temperature. The cells were rinsed with PBS twice and pretreated with PBS containing 0.3% Triton -X100 for 5 min at room temperature. After blocking in TNB buffer (Provided by NEN™ Life Science Products, Inc.) for 1 h at room temperature, the cells were incubated at 4°C overnight with the following antibodies: anti-Nestin (Rat-401, mouse IgG, 1:200), anti-Islet-1/2 (40.2D6, mouse IgG, 1:500), anti-Lim3 (67.4E12, mouse IgG, 1:1000), anti-HB9 (81.5C10, mouse IgG, 1:100), anti-Otx1 (Otx-5F5, mouse IgG, 1:500000), anti-Nkx2.2 (74.5A5, mouse IgG, 1:5000), anti-Pax7 (mouse IgG, 1:5000) (Developmental Studies of Hybridoma Bank: DSHB), anti-βIII-tubulin (mouse IgG, 1:1000, Sigma T8660), anti-Olig2 (rabbit IgG, 1:30000) (Mizuguchi et al., 2001; Takebayashi et al., 2000), anti-Phox2b (rabbit IgG, 1:25000) (Pattyn et al., 1997), anti-Nkx6.1 (Ab174.3, rabbit IgG., 1:200000) (Jensen et al., 1996), anti-Group B1 Sox [Sox1/(2)/3] (rabbit IgG, 1:10000) (Tanaka et al., unpublished). Anti-Group B1 Sox [Sox1/(2)/3] antibody is weakly reactive with Sox2, which is expressed not only by the neural primordium but by undifferentiated ES cells, and with Sox1 and Sox3 (with preference for Sox1 and Sox3 over Sox2). However, as all Group B1 Sox genes are expressed in neural primordium (Wood and Episkopou, 1999), we used this antibody to detect neural progenitors, by determining the immunostaining conditions under which undifferentiated ES cells, which were used as a negative control, did not stain (data not shown). Antigen retrieval was accomplished by incubating the samples in the boiled PBS for 10 min for anti-Isl-1/2 and anti-Lim3, in boiled Target Retrieval Solution (DAKO) for 10 min for anti-Nkx2.2, or in 1 N HCl at 30°C for 15 min for anti-Pax7. After washing with PBS three times, the cells were incubated for 1 h at room temperature with secondary antibodies conjugated with Alexa 488 or Alexa 568 (Molecular Probes). For anti-Islet1/2, anti-Lim3, anti-HB9, anti-Olig2, anti-Phox2b, anti-Otx1, anti-Nkx2.2, anti-Pax7, and anti-Nkx6.1 staining, we used biotinylated secondary antibodies (Jackson Immunoresearch Laboratory, Inc.) after exposure to 1% H_2O_2 for 15 min at room temperature to inactivate endogenous peroxidase. The signals were then enhanced with streptavidin-HRP (SA-HRP), followed by TSA™ Fluorescein System (NEN™ Life Science Products, Inc.). After washing with PBS, the samples were mounted on slides and examined with a universal fluorescence microscope (Axiophot 2, Carl Zeiss) and a confocal laser scanning microscope (LSM510, Carl Zeiss). The nuclei of all samples were stained with hoechst33342 (1 μg/ml, Sigma B2261). For statistical analysis, at least 200 cells per cover glass were examined, and the numbers of cells that had immunoreacted with each antibody were counted and expressed as a percentage of the total number of cells whose nuclei stained with hoechst33342. The *P* values for statistical significance (*t* test) are stated in the figure legends.

Western blot analysis

Western blot analysis was performed by the previously established method. A 20 μg protein sample of a total cell extract was run on 7.5–15% SDS-PAGE, transferred to nitrocellulose, and probed with each antibody. The blot was probed with the following antibodies: anti-Nestin (Rat-401, mouse IgG, Developmental Studies of Hybridoma Bank: DSHB), anti-βIII-tubulin (mouse IgG, Sigma T8660), anti-Glial Fibrillary Acidic Protein (GFAP) (rabbit IgG, DAKO Z0334), anti-CNPase (mouse IgG, Sigma C5922), and anti-Shh N-terminal fragment (goat IgG, Santa Cruz sc-1194). Signals were detected with HRP-conjugated secondary antibodies (Jackson Immunoresearch Laboratory, Inc.) by using an ECL kit (Amersham Biosciences). Quantitative analysis was performed with Scion Image (Scion Corpo-

ration). The amounts of proteins loaded in each slot were normalized to those of α-tubulin.

RNA isolation and RT-PCR

RT-PCR analysis of at least two independent cultures was performed in most of the experiments, and were similar results obtained. Total RNA was isolated with Trizol reagent (Invitrogen™ 15596-018) and DNase I treatment, or by the RNeasy Mini Kit (Qiagen). Total RNA (1–3 μg) was used to synthesize cDNA with 500 ng oligo-d$(T)_{12-18}$ primers. The cDNA synthesis was performed at 42°C for 50 min in a final volume of 20 μl according to the manufacturer's instructions for Superscript II RNase H^- reverse transcriptase (Invitrogen™). To analyze relative expression of different mRNAs, the amount of cDNA was normalized based on the signals from ubiquitously expressed *β-actin* mRNA. The PCR was carried out by using a KOD Plus kit (Toyobo) according to the manufacturer's standard protocol in a final volume of 25 μl. Primer sequences and PCR cycling conditions will be provided upon request. To provide negative controls and exclude contamination by genomic DNA, the reverse transcriptase was omitted in the cDNA synthesis step, and the samples were subjected to the PCR reaction in the same manner with primer sets for *β-actin*, and are indicated at the bottom of each figure as RT(−). PCR products were electrophoresed in agarose gel, and bands were visualized with ethidium bromide under UV light. The identity of the PCR products was confirmed by sequencing.

Results

Differentiation potential of mouse ES cells regulated by RA

RA has been shown to be one of the most important extrinsic morphogens and precisely modulates the differentiation properties of ES cells into various cell types, including neural cells, skeletal muscle cells, adipocytes, cardiomyocytes, and vascular smooth muscle cells, in an incubation-time- and concentration-dependent manner (Rohwedel et al., 1999). To examine the concentration-dependent effects of RA on the differentiation of ES cells, we first differentiated ES cells by inducing the formation of EBs in the presence of various concentrations of RA. We also used Noggin, a secreted protein that plays a role in neural induction by inhibiting BMP-signaling (Finley et al., 1999; Gratsch and O'Shea, 2002; Kawasaki et al., 2000; Smith and Harland, 1992; Tropepe et al., 2001; Zimmerman et al., 1996), to investigate RA-independent neural differentiation. ES cells were plated onto bacteriological dishes and had been cultured for 6 days in medium containing various concentrations of RA (added on day 2) or xNoggin conditioned medium (Fig. 1), and they were analyzed by RT-PCR for markers of the three primary germ layers

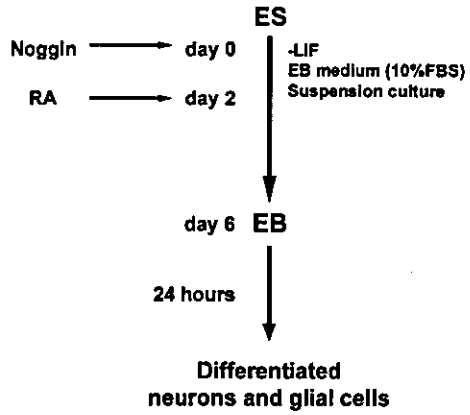

Fig. 1. Experimental protocol for differentiation of ES cells with retinoic acid (RA) or xNoggin conditioned medium. ES cells were cultured in the bacteriological dish for 6 days and formed embryoid bodies (EBs). Various concentrations of RA were added on day 2 of EB formation. Then, EBs were dissociated and differentiated on poly-L-ornithine/fibronectin-coated cover glasses.

(Fig. 2). On day2, *oct3/4*, which is a marker for undifferentiated ES cells, was expressed by both control and Noggin-treated EBs. From day 4 of EB formation onward, *oct3/4* expression was gradually down-regulated by RA in a concentration-dependent manner and in a culture period-dependent manner, and it became undetectable on day 6 under all conditions, indicating that most of the ES cells had differentiated by 6 days of EB formation. On day 6, expression of *ck-17 (cytokeratin 17)*, a marker of epidermis (McGowan and Coulombe, 1998), and expression of *ngn2*, which is expressed in neuronal progenitors (Mizuguchi et al., 2001; Novitch et al., 2001; Ross et al., 2003), were enhanced by high-concentration RA treatment ($>10^{-7}$ M; high-RA), and thus ectodermal differentiation was promoted by exposure to high-RA. Expression of *ck-17* mRNA in undifferentiated ES cells, which also expressed *oct3/4* (Fig. 2), was also demonstrated in a previous study (Tropepe et al., 2001). In the control, Noggin, and low-RA-treated EBs, its expression coincided with expression of *oct3/4* at day 4, and was then down-regulated by day 6 along with extinction of *oct3/4*. In the high-RA-treated EBs, on the other hand, expression of *ck-17* mRNA was detected at day 4 and day 6, without expression of *oct3/4*. The expression of *ck-17* in the absence of expression of *oct3/4* can be understood as indicating promotion of epidermal differentiation in EBs treated with high-RA. Mesodermal differentiation, represented by expression of *brachyury*, which is essential for the formation and organization of mesoderm (Herrmann et al., 1990; Wilkinson et al., 1990), and expression of homeobox gene *nkx2.5*, the earliest known marker of cardiac development (Komuro and Izumo, 1993; Lints et al., 1993), were facilitated by low-concentration RA treatment (10^{-9}–10^{-8} M; low-RA). Endodermal markers, including *gata4*, expressed in primitive endoderm (Arceci et al., 1993), and *pdx1*, expressed in developing pancreas (Jonsson et al., 1994; Offield et al., 1996), were

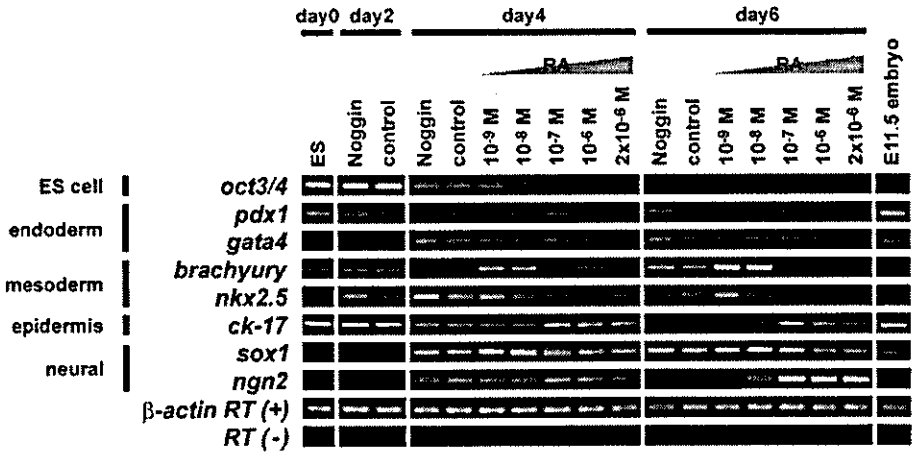

Fig. 2. Expression of markers of the three primary germ layers in EBs exposed to various concentrations of RA. RNA was isolated from ES cells (day 0) and EBs (days 2, 4, 6) and analyzed by RT-PCR for expression of markers of undifferentiated ES cells (*oct3/4*), endoderm differentiation (*pdx1* and *gata4*), mesoderm differentiation (*brachyury* and *nkx2.5*), epidermis differentiation (*ck-17*), and neural differentiation (*sox1* and *ngn2*). To normalize their expression to the amount of cDNA present in the sample, the cDNA for endogenous *β-actin* was amplified.

expressed unstably at low levels, and their levels correlated poorly with the concentrations of RA.

Neural induction of mouse ES cells by RA

It has been shown that neural differentiation of ES cells can be promoted by RA, especially by early exposure of EBs to relatively high RA concentrations (Bain et al., 1995, 1996; Fraichard et al., 1995; Gajovic et al., 1997; Renoncourt et al., 1998; Rohwedel et al., 1999; Strubing et al., 1995; Wichterle et al., 2002). However, as the effect of different RA concentrations had never been precisely described, we next investigated how RA promotes neural differentiation. EBs that had been cultured for 6 days were analyzed for differentiation markers of neural cells (progenitors, neurons, and glia) by Western blotting (Figs. 3A, B). Nestin, which is expressed in undifferentiated neural progenitors, was more strongly expressed in EBs treated with low-RA. Expression of βIII-tubulin and GFAP, which are markers of differentiated neurons and astrocytes, respectively, increased in a concentration-dependent manner in EBs exposed to RA (Figs. 3A, B). By contrast, RT-PCR analysis on day 6 showed that expression of *sox1* (a marker of undifferentiated neural cells; Pevny et al., 1998; Wood and Episkopou, 1999) mRNA was higher in EBs treated with low-RA on day 6 (Fig. 2). Expression of CNPase, a marker of oligodendrocytes, was detected only slightly under all of the differentiating conditions, and its expression was not very strongly affected by the concentration of RA (Figs. 3A,B). To better understand the effects of RA on neural differentiation of EBs, we performed immunocytochemistry of markers of various neural lineages (Figs. 3C–E and 5A,B). EBs that had been cultured for 6 days were dissociated and differentiated on poly-L-ornithine/fibronectin-coated cover glasses for 24 h and then processed for immunocytochemistry of markers of undifferentiated neural cells (Nestin, Group B1 Sox, Olig2) and postmitotic neurons (βIII-tubulin). Olig2 is a basic-helix-loop-helix (bHLH) transcription factor that is expressed in most of the ventral neural progenitor cells around the period of neural tube closure (Takebayashi et al., 2000). Treatment of EBs with low-RA (10^{-8} M) induced a 1.6-, 3.0-, and 9.1-fold increase in Nestin-, Group B1 Sox, and Olig2-positive undifferentiated neural progenitors, respectively, over those treated with high-RA (2×10^{-6} M) (Figs. 3C–E). Treatment of EBs with high-RA (2×10^{-6} M) induced very few Nestin-, Group B1 Sox-, and Olig2-positive progenitor cells, and instead induced many βIII-tubulin-positive postmitotic neurons [3.0-fold more than by treatment with low-RA (10^{-8} M)] (Figs. 3C–E and 5A). RT-PCR analysis showed that *olig2* was expressed in EBs treated with high-RA at day 4 and down-regulated by day 6, whereas it was expressed highly on day 6 in EBs treated with low-RA (Fig. 6A). These results indicate that higher concentrations of RA facilitate differentiation of neural progenitors into postmitotic neurons and glia, in contrast to lower concentrations of RA, which preferentially induce undifferentiated neural progenitor cells from ES cells; that is, that RA strongly promotes terminal differentiation of ES-cell-derived neural progenitors in a concentration- and culture-period-dependent manner in addition to its action that promotes neural induction of ES cells.

ES-cell-derived neural cells acquire positional identity through EB formation

To investigate how RA regulates the specification of rostro-caudal and dorso-ventral positional identity during EB formation, RT-PCR analysis of regionally specific markers was performed (Carpenter, 2002; Caspary and Anderson, 2003; Helms and Johnson, 2003; Hitoshi et al., 2002; Jessell, 2000; Marquardt and Pfaff, 2001;

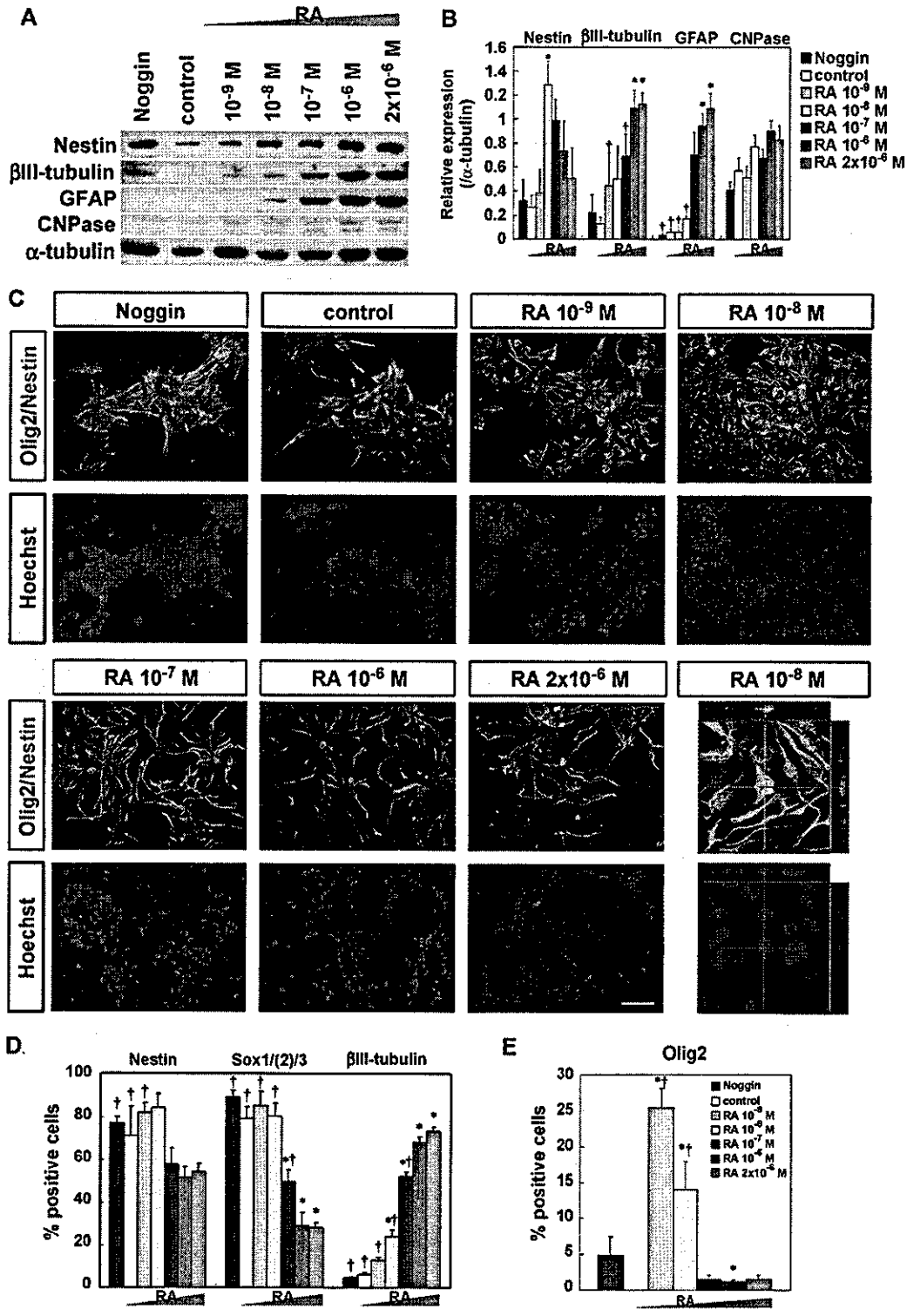

Fig. 3. RA promotes neural differentiation in a concentration-dependent manner and regulates the differentiation of ES-cell-derived neural progenitors. (A) Western blot analysis of markers for neural differentiation in EBs cultured for 6 days. (B) Quantitative analysis was performed with Scion Image. The amounts of proteins were normalized to those of α-tubulin ($n = 3$, mean ± SEM, *, $P < 0.05$ vs. control. †, $P < 0.05$ vs. RA 2×10^{-6} M). (C) Immunocytochemistry of dissociated EBs for Olig2 and Nestin. Nuclear localization of Olig2 in Nestin immunoreactive cells was confirmed by three-dimensional reconstruction of confocal microscopic images (right end of lower panels). (D, E) The proportions of cells positive for Nestin, Group B1 Sox, Olig2, and βIII-tubulin among the total number of cells in dissociated EBs were determined by immunocytochemically. Immunoreactive cells as a percentage of the total number of cells counted on the basis of nuclear staining with hoechst33342 are shown ($n = 3$, mean ± SEM, *, $P < 0.05$ vs. control. †, $P < 0.05$ vs. RA 2×10^{-6} M). The percentages of cells expressing Olig2, Group B1 Sox, and Nestin were higher in dissociates of EBs treated with low-RA ($<10^{-8}$ M) than in EBs treated with high-RA ($>10^{-7}$ M). Scale bar: 50 μm.

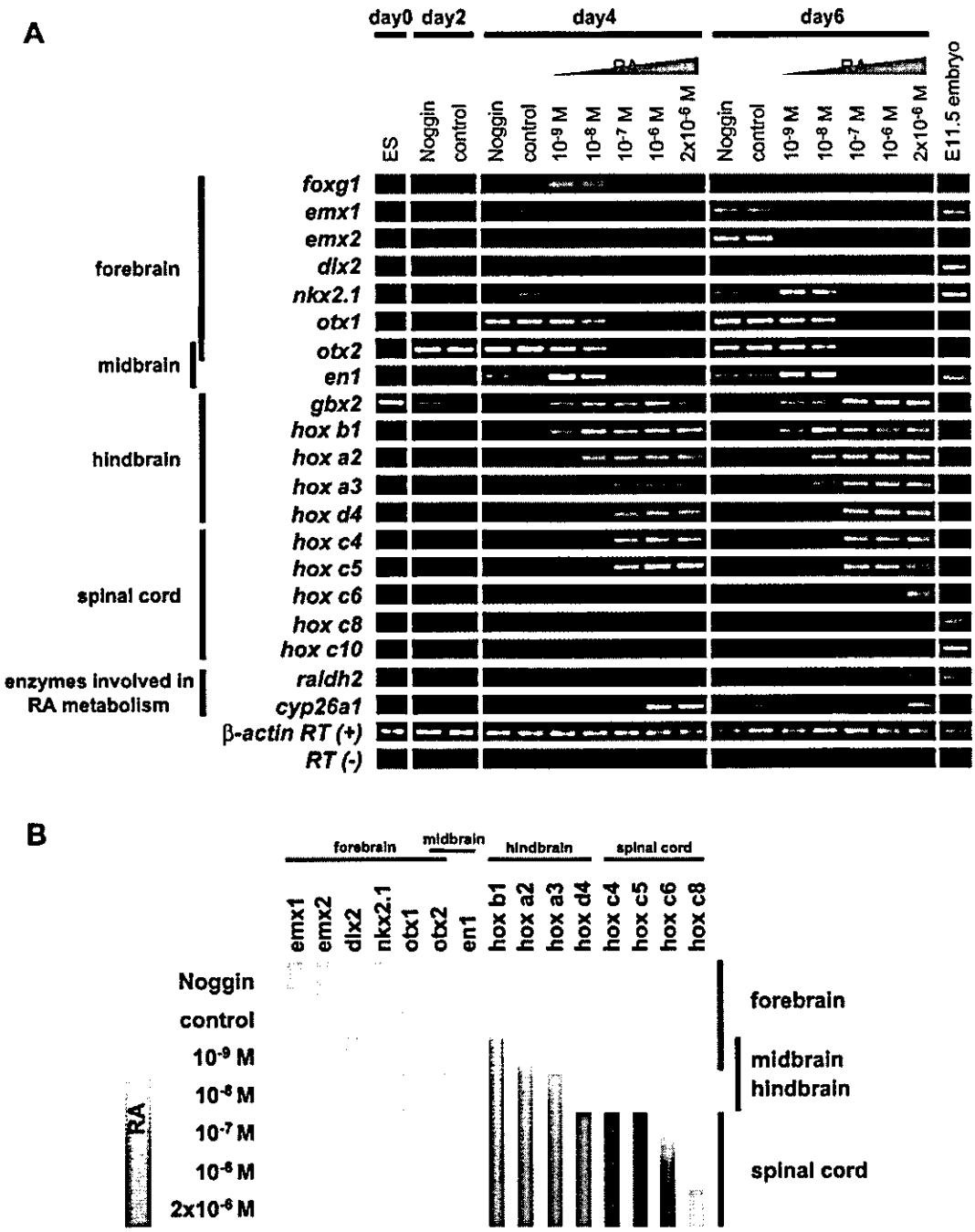

Fig. 4. Concentration-dependent effects of RA on the specification of rostrol-caudal positional identity of ES-cell-derived neural progenitors. (A) Effect of RA on rostrol-caudal axis formations was analyzed by RT-PCR on days 0, 2, 4, and 6 of differentiation. The expression patterns are summarized in (B). RA caudalized ES-cell-derived neural cells in a concentration-dependent manner. Control and Noggin-treated-EBs expressed forebrain-type markers, whereas EBs treated with low-RA and high-RA expressed midbrain–hindbrain-type markers and spinal-cord-type markers, respectively.

Fig. 5. RA caudalizes EB-derived neurons in a concentration-dependent manner. (A) Immunocytochemical analysis of neural progenitors and neurons differentiated from dissociated EBs with Otx1, which is expressed in developing forebrain and midbrain, and Phox2B, Lim3, HB9, and Isl-1/2, which are expressed in developing motor neurons and their progenitors. Immunoreactive cells as a percentage of the total number of cells counted on the basis of the nuclear staining with hoechst33342 are shown in B ($n = 3$, mean ± SEM, *, $P < 0.05$ vs. control. †, $P < 0.05$ vs. RA 2×10^{-6} M). (C) RT-PCR analysis of *phox2b* and *hb9*. Control and Noggin-treated EBs generated significant numbers of Otx1-and Group B1 Sox-positive anterior neural progenitors. Low-RA (10^{-9}–10^{-8} M) induced many Phox2b-positive hindbrain brachial and visceral motor neurons and fewer Otx1/Group B1 Sox-positive anterior neural progenitors, whereas high-RA (>10^{-7} M) induced more HB9-positive hindbrain and spinal cord somatic motor neurons without any Otx1-positive cells. Scale bar: 50 μm.

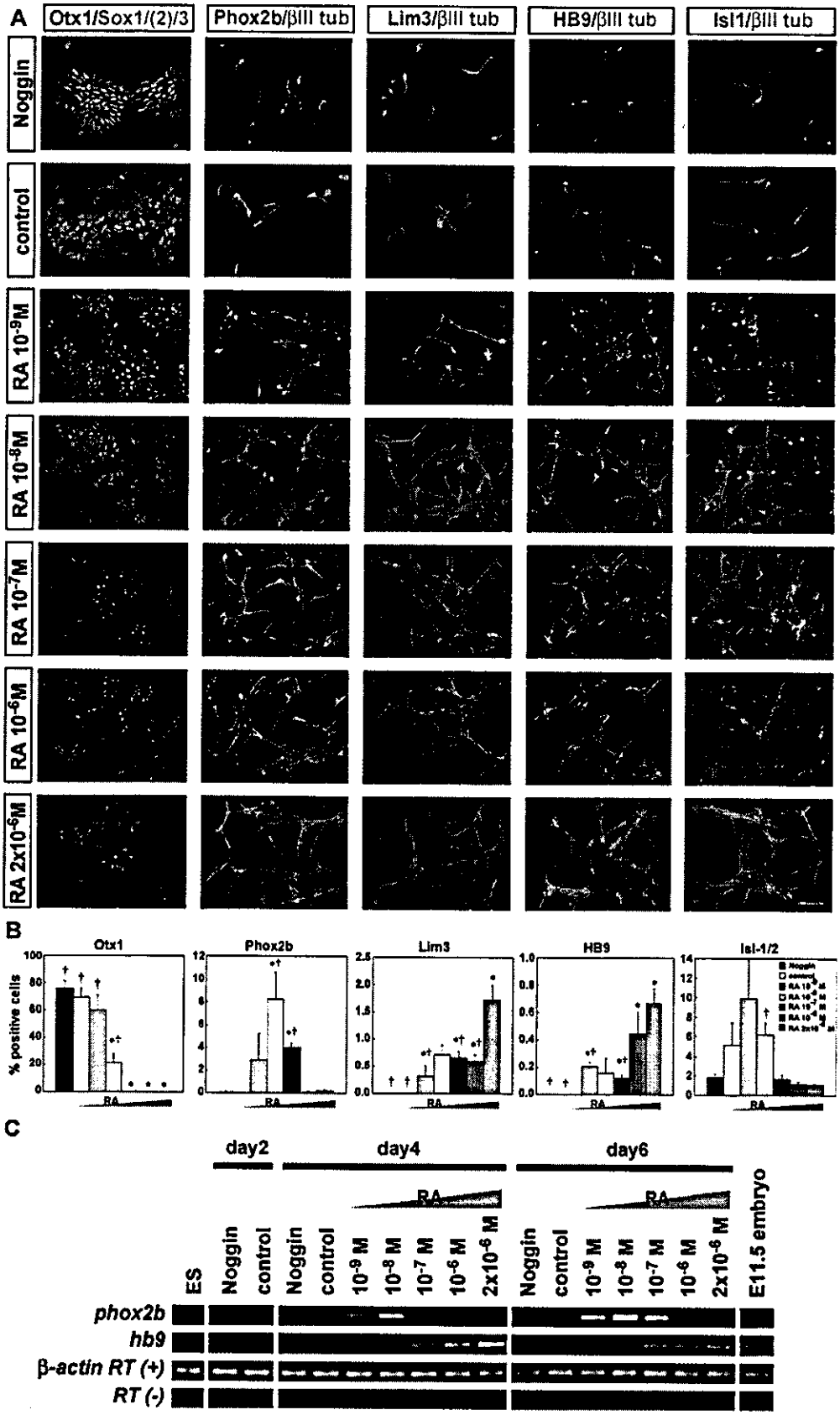
A
Otx1/Sox1/(2)/3
Phox2b/βIII tub
Lim3/βIII tub
HB9/βIII tub
Isl1/βIII tub
Noggin
control
RA 10-9M
RA 10-8M
RA 10-7M
RA 10-6M
RA 2x10-6M
B
Otx1
Phox2b
Lim3
HB9
Isl-1/2
% positive cells
RA
C
day2
day4
day6
RA
ES
Noggin
control
10-9 M
10-8 M
10-7 M
10-6 M
2x10-6 M
E11.5 embryo
phox2b
hb9
β-actin RT (+)
RT (-)

Niederreither et al., 2000; Schuurmans and Guillemot, 2002; Wurst and Bally-Cuif, 2001). As shown in Fig. 4, EBs were caudalized in a concentration-dependent manner during the first 2 days of RA exposure (days 2–4). After day 4, control and Noggin-exposed EBs expressed genes specific to forebrain (*emx1*, *emx2*, *nkx2.1*, *otx1*, *otx2*) and midbrain–hindbrain (*otx1*, *otx2*, *en1*), but no hindbrain or spinal cord markers. EBs treated with low-RA mainly expressed midbrain–hindbrain markers (*otx1*, *otx2*, *en1*, *gbx2*, *hoxb1*, *hoxa2*, *hoxa3*), and did not express spinal cord markers (*hoxc4*, *hoxc5*, *hoxc6*, *hoxc8*, *hoxc10*). Expression of telencephalic markers (*emx1*, *emx2*, *dlx2*) in EBs treated with low-RA was lower than in control and Noggin-exposed EBs. However, at day 4, expression of one of the telencephalic markers, *foxg1*, was somehow highest in the EBs exposed to low-RA. On the other hand, high-RA induced expression of hindbrain and rostral spinal cord markers (*hoxc4*, *hoxc5*, *hoxc6*) and reduced expression of forebrain and midbrain markers. These patterns of gene expression were detected at day 4 and were maintained thereafter. The expression levels of enzymes involved in RA metabolism, *raldh2* and *cyp26a1* (Fig. 4A), were higher in EBs treated with high-RA, a finding that was consistent with the EBs exposed to high-RA acquiring the identity of rostral spinal cord, where the concentration of RA and the expression level of its synthesizing enzyme Raldh2 are the highest in the developing CNS (Swindell et al., 1999). The RA catabolizing enzyme Cyp26a1 may have been induced by high-RA as part of a negative feedback mechanism. The total gene expression patterns indicating rostro-caudal specification in EBs differentiated under different conditions are summarized in Fig. 4B. The concentration-dependent caudalization of EBs by RA treatment shown by the result of the RT-PCR analysis was confirmed by immunocytochemistry of dissociated EBs with antibodies for markers expressed in developing forebrain and midbrain (Otx1) (Acampora et al., 1998), visceral or brachial motor neurons in the hindbrain (Phox2b) (Pattyn et al., 2000), and somatic spinal motor neurons (HB9, Lim3) (Arber et al., 1999) (Figs. 5A,B). Virtually all of the marker-positive cells were also positive for either a neural progenitor marker Group B1 Sox, or pan-neuronal marker βIII-tubulin. A significant number of cells derived from EBs and grown under all conditions expressed Isl-1/2, a marker of postmitotic cholinergic neurons, including not only spinal motor neurons but those in ventral forebrain (Kohtz et al., 2001; Wang and Liu, 2001). Somatic motor neurons of the hindbrain and spinal cord expressing Lim3 and HB9 were found more frequently when treated with high-RA, whereas hindbrain visceral or brachial motor neurons expressing Phox2b were found more frequently when treated with low-RA. By contrast, an enormous number of neural progenitors that were positive for both Otx1 and Group B1 Sox and acquired anterior positional identity were induced from control and Noggin-treated EBs, and less frequently from low-RA treated EBs, whereas no such cells were induced from high-RA-treated EBs. Taken together, these findings indicate that RA induced both caudalization of EBs based on the expression patterns of regionally specific genes during neural induction and neuronal differentiation in a concentration-dependent manner, resulting in significant generation of forebrain and midbrain (control and Noggin), hindbrain (low-RA), and spinal cord (high-RA) types of neural progenitors or neurons, respectively.

RA controls dorso-ventral axis formation

To determine the effect of RA on dorso-ventral axis specification of EB-derived cells, we investigated the expression of class I genes (*pax7*, *dbx1*, *dbx2*, *irx3*, *pax6*, whose expression is *repressed* by Shh in early CNS development) and class II genes (*nkx6.2*, *nkx6.1*, *olig2*, *nkx2.2*, whose expression is *activated* by Shh). These genes are differentially expressed along the dorso-ventral axis in the progenitor domains of developing hindbrain and spinal cord (Jessell, 2000). As shown in Fig. 6, EBs treated with low-RA expressed both class I and class II genes, indicating that they were composed of various populations that had acquired their identities throughout the dorsal to ventral neural tube. Interestingly, on the other hand, treatment with high-RA raised the expression levels of class I genes and significantly reduced those of class II genes except *olig2* at day 4, in comparison to treatment with low-RA. Thus, high-RA caused dorsalization of neural progenitor cells in EBs. To investigate the mechanism underlying the action of RA in specifying dorso-ventral identity, we investigated its effects on expression of the N-terminus of Shh protein (Shh-N) and *sonic hedgehog* (*shh*) mRNA. Mouse Shh is produced as a 49-kDa secreted protein that post-translationally cleaves to yield two mature proteins: an approximately 19-kDa N-terminal fragment that contains the signaling portion of the molecule and an approximately 27-kDa C-terminal fragment, which has auto-processing activity (Marti et al., 1995; Porter et al., 1995, 1996; Roelink et al., 1995). We found that expression of both the Shh-N protein and *shh* mRNA was significantly up-regulated by exposure to low-RA in day 4–6 EBs (Figs. 7A–C), but that further increasing the RA concentration ($>10^{-7}$ M) induced their down-regulation instead. More specifically, the RA-responsive increase in Shh-N expression appeared to be concentration-dependent up to 10^{-8} M, but was completely abrogated at 10^{-7} M and higher concentrations. On the other hand, the peak level of full-length Shh protein expressed in response to exposure to 10^{-8} M of RA was maintained even in EBs exposed to higher concentrations of RA. These results suggested that the ventralization of neural progenitors in EBs exposed to low-RA might be caused by an enhanced expression of Shh-N. However, we

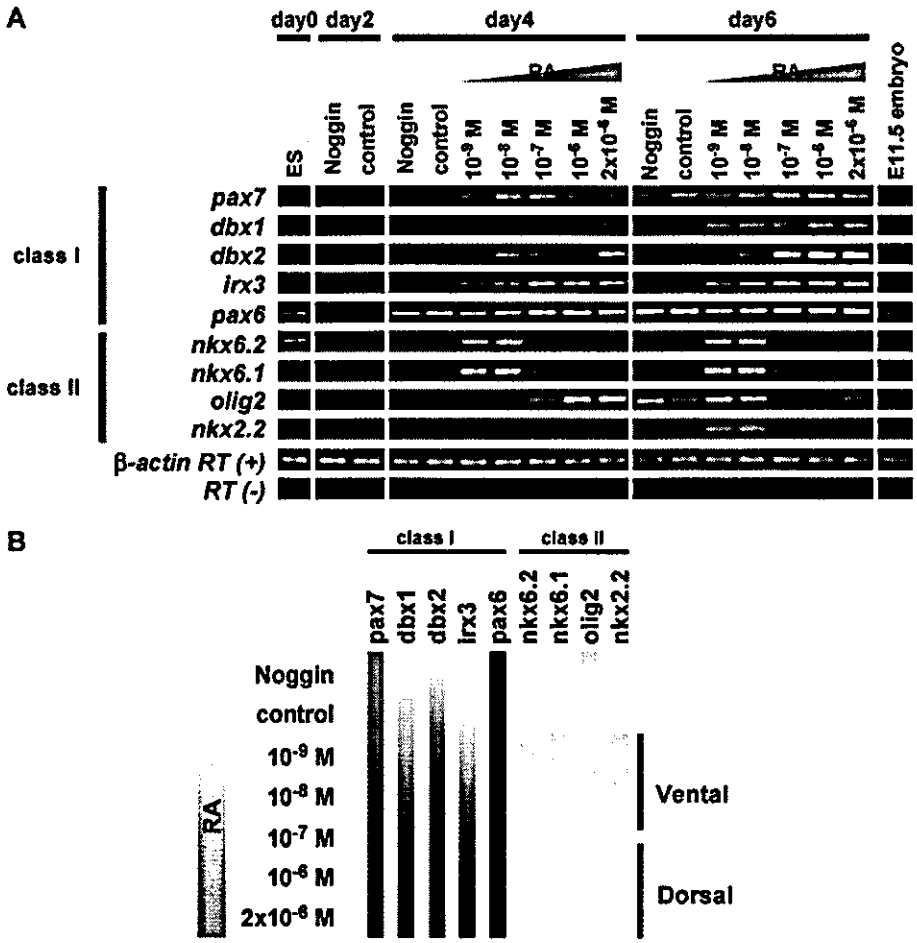

Fig. 6. Specification of the dorso-ventral identity of ES-cell-derived neural progenitors is regulated by RA. (A) RT-PCR analysis of class I and class II genes, which define dorsol-ventral positional identity. The expression patterns are summarized in (B). EBs treated with low-RA (10^{-9}–10^{-8} M) expressed both class I and II genes (class II > class I), which indicated that both ventral and dorsal neural progenitors had been induced, whereas EBs treated with high-RA (>10^{-6} M) expressed only class I gene, indicating dorsal neural progenitors had been induced.

could not rule out the possibility of the opposite causal relationship; that is, that low-RA induced enhanced expression of Shh-N protein and the expression of *shh* mRNA resulted from the ventralization of EB-derived cells that had been induced by low-RA treatment through an unknown mechanism. To address this issue, we treated EBs exposed to RA with recombinant Shh-N protein and cyclopamine, an inhibitor of Shh signaling (Chen et al., 2002a,b; Incardona et al., 1998). In the absence of cyclopamine treatment, EBs exposed to low-RA expressed both class I (*pax7*, *dbx1*, *dbx2*, *irx3*, and *pax6*) and class II genes (*nkx6.2*, *nkx6.1*, *olig2*, and *nkx2.2*), thereby indicating both dorsal and ventral phenotype. Treatment with 1 μM cyclopamine strongly down-regulated the ventral class II genes (*nkx6.2*, *nkx6.1*, *olig2*, and *nkx2.2*) and some of the class I genes (*dbx1* and *dbx2*), indicating a dorsalized phenotype (Figs. 7D,E). In addition, exposure to 50 nM of recombinant Shh-N protein enhanced expression of class II genes (*nkx6.2*, *nkx6.1*, *olig2*, and *nkx2.2*) but reduced *pax7* expression. These effects were abrogated by treatment with 1 μM cyclopamine (Figs. 7D,E). EBs treated with high-RA expressed higher levels of class I genes (*pax7*, *dbx1*, and *dbx2*, *irx3*, *pax6*), but lower levels of class II genes (*nkx6.2*, *nkx6.1*, *olig2*, and *nkx2.2*), thereby indicating a more dorsal phenotype than after low-RA treatment. However, high-RA treated EBs were ventralized by treatment with exogenous Shh-N, as shown by the up-regulation of class II genes (*nkx6.2*, *nkx6.1*, *olig2*, and *nkx2.2*) and down-regulation of *pax7*, and these changes were also abrogated by 1 μM cyclopamine treatment (Figs. 7D,E).

This alteration of dorso-ventral identity by RA, Shh-N, and cyclopamine was confirmed by the immunostaining of dissociated EBs with antibodies against Pax7, Nkx6.1, and Nkx2.2 (Fig. 8). Virtually all the marker-positive cells also stained with the antibodies against Group B1 Sox or Nestin, indicating they are neural progenitor cells. It was noteworthy that Shh-N treatment could induce only Nkx6.1-positive but not Nkx2.2-positive neural progenitors in EBs treated with high-RA, indicating that the ventralmost neural progenitors could not be efficiently derived under such conditions, but that they were capable of increasing the